

Review

Organocatalysis: A Tool of Choice for the Enantioselective Nucleophilic Dearomatization of Electron-Deficient Six-Membered Ring Azaarenium Salts

Claire Segovia, Pierre-Antoine Nocquet, Vincent Levacher , Jean-François Brière  and Sylvain Oudeyer 

Normandie University, UNIROUEN, INSA Rouen, CNRS, COBRA, 76000 Rouen, France; claire.segovia@insa-rouen.fr (C.S.); vincent.levacher@insa-rouen.fr (V.L.); jean-francois.briere@insa-rouen.fr (J.-F.B.)

* Correspondence: sylvain.oudeyer@univ-rouen.fr; Tel.: +33-235522496

Abstract: Nucleophilic dearomatization of azaarenium salts is a powerful strategy to access 3D scaffolds of interest from easily accessible planar aromatic azaarene compounds. Moreover, this approach yields complex dihydroazaarenes by allowing the functionalization of the scaffold simultaneously to the dearomatization step. On the other side, organocatalysis is nowadays recognized as one of the pillars of the asymmetric catalysis field of research and is well-known to afford a high level of enantioselectivity for a myriad of transformations thanks to well-organized transition states resulting from low-energy interactions (electrostatic and/or H-bonding interactions . . .). Consequently, in the last fifteen years, organocatalysis has met great success in nucleophilic dearomatization of azaarenium salts. This review summarizes the work achieved up to date in the field of organocatalyzed nucleophilic dearomatization of azaarenium salts (mainly pyridinium, quinolinium, quinolinium and acridinium salts). A classification by organocatalytic mode of activation will be disclosed by shedding light on their related advantages and drawbacks. The versatility of the dearomatization approach will also be demonstrated by discussing several chemical transformations of the resulting dihydroazaarenes towards the synthesis of structurally complex compounds.

Keywords: organocatalysis; dearomatization reactions; asymmetric catalysis



Citation: Segovia, C.; Nocquet, P.-A.; Levacher, V.; Brière, J.-F.; Oudeyer, S. Organocatalysis: A Tool of Choice for the Enantioselective Nucleophilic Dearomatization of Electron-Deficient Six-Membered Ring Azaarenium Salts. *Catalysts* **2021**, *11*, 1249. <https://doi.org/10.3390/catal11101249>

Academic Editor: Luca Bernardi

Received: 28 September 2021

Accepted: 16 October 2021

Published: 18 October 2021

Publisher's Note: MDPI stays neutral with regard to jurisdictional claims in published maps and institutional affiliations.



Copyright: © 2021 by the authors. Licensee MDPI, Basel, Switzerland. This article is an open access article distributed under the terms and conditions of the Creative Commons Attribution (CC BY) license (<https://creativecommons.org/licenses/by/4.0/>).

1. Introduction

Dihydropyridines and their azaarene counterparts like dihydroisoquinolines, dihydroquinolines and dihydroacridines are widespread backbones in naturally occurring products or drugs and are interesting building blocks for the construction of complex architectures (Figure 1a) [1]. For example, 1,4-dihydropyridines are present in the well-known NAD (nicotinamide adenine dinucleotide), a co-enzyme found in living cells which exists under two red-ox forms (NAD^+/NADH), in the so-called Hantzsch ester, a useful hydride transfer reagent in organic synthesis, or in Nifedipine, a drug used for the treatment of hypertension. Although less stable, 1,2-dihydropyridines were reported as useful reactive building blocks, for example in the synthesis of (–)-Oseltamivir (Tamiflu®), a drug used in the treatment of influenza [2]. Therefore, several strategies were developed for the enantioselective synthesis of these scaffolds based upon two major approaches (Figure 1b). The first one involving the construction of the dihydroazaarenes, a strategy that will not be covered in this review [3–6]. The second one involves the dearomatization of azaarenes by nucleophilic addition or reduction (addition of hydride) to the corresponding azaarenium salt. Dearomatization is very appealing since it produces 3D scaffolds from readily available aromatic precursors. Whereas enantioselective hydride addition requires the use of pre-functionalized azaarenes (introduction of Nu prior to the addition of the hydride) and leads to tetrahydro products (and therefore will not be discussed herein) [7–9], nucleophilic dearomatization ($\text{Nu} \neq \text{H}$) offers the advantage of introducing chemical diversity

simultaneously to the dearomatization step. Nevertheless, the azaarenes suffer from poor electrophilicity and thus generally require an activation step to undergo a nucleophilic addition (Figure 1c). The activation step can occur by introducing a carbamate on the nitrogen of the azaarene to afford the corresponding azaarenium as more electrophilic species. As far as *N*-alkyl azaareniums are concerned, the introduction of an extra electron-withdrawing group at the C3 position is generally mandatory to ensure good reactivity towards a wide array of nucleophiles. Moreover, azaarenium salts exhibit two different electron-deficient sites at positions C2 (mainly for pyridinium, isoquinolinium and quinolinium salts) and C4 (mainly for pyridinium, quinolinium or acridinium salts). The regioselectivity of the addition is related to the HSAB theory, hard nucleophiles generally add at the C2 position whereas soft nucleophiles add to the C4 position [10], albeit the catalyst might also influence this issue.

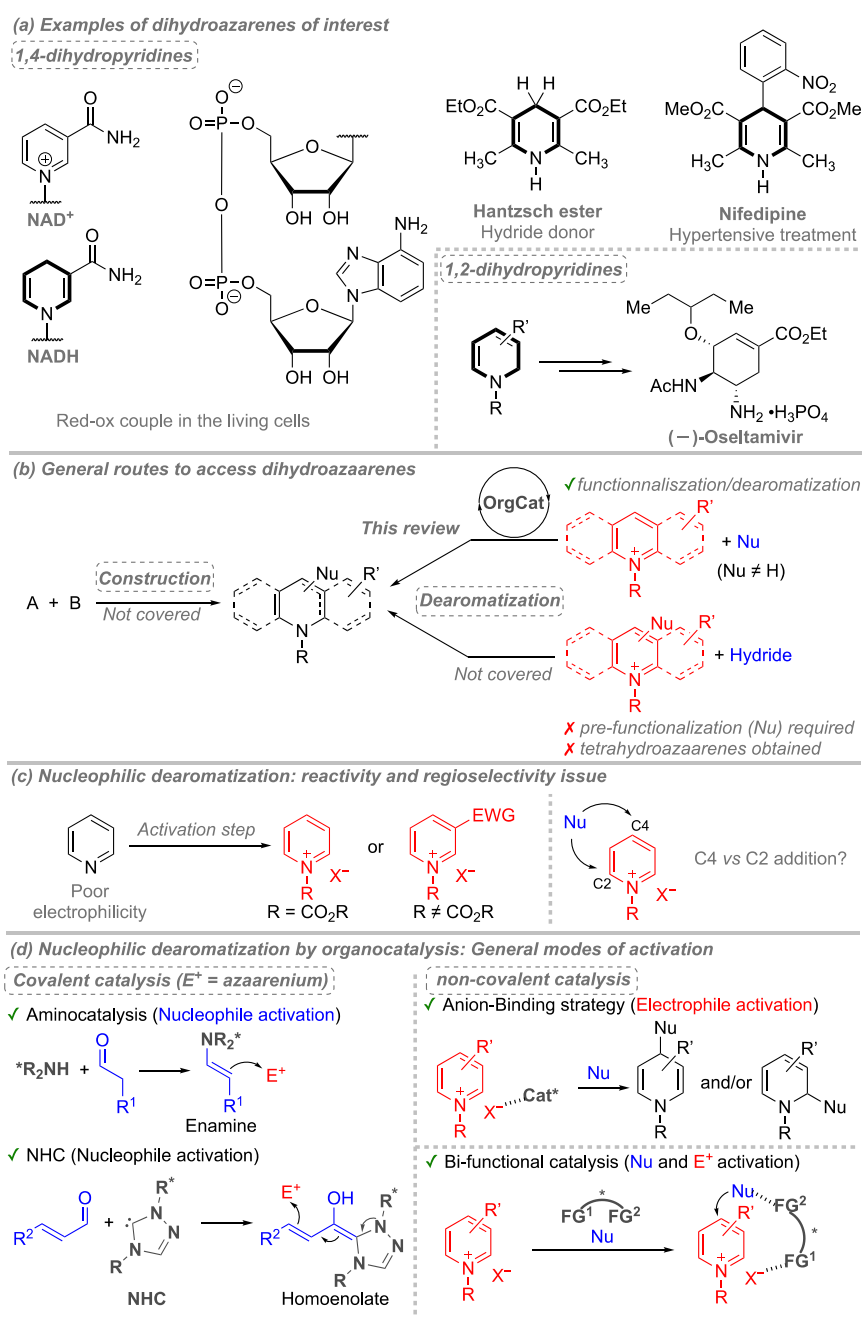


Figure 1. Dearomatization of azaarene: general considerations. * was used to indicate that catalysts are chiral.

Taking into account the above-mentioned challenges, enantioselective nucleophilic dearomatization of azaarenium salts has attracted a great deal of attention mostly by using metal catalysts with chiral ligands [11–20]. Nevertheless, in the last fifteen years and due to the advent of organocatalysis [21–36], which was recently highlighted through the Nobel Prize of Prof. B. List and Prof. D. MacMillan, several enantioselective organocatalytic dearomatization reactions of azaarenium salts have been reported [11,13–16,18,19,37,38]. Organocatalysts can be classified following the mode of activation of either the electrophilic and/or nucleophilic partners involved in a given reaction [24,25]. Activation can be performed through covalent and/or noncovalent interactions with the substrates (Figure 1d). As far as non-covalent interactions are concerned, anion binding or H-bonding interactions can be achieved thanks to chiral (thio)urea or oligotriazole catalysts for instance. Covalent catalysis generally involves chiral primary or secondary amines (also known as aminocatalysis) or *N*-heterocyclic carbenes (NHC) catalysts. Whatever the type of catalysts, well-organized transition states are favored by low energy interactions (coulombic or H-bonding interactions) and eventually enhanced by at least two modes of activation occurring simultaneously thanks to the so-called bifunctional organocatalysis results in a high level of enantioselectivity [39]. These unique features of organocatalysis are of particular interest in order to better control the regioselectivity of the enantioselective nucleophilic addition to azaarenium salts along with affording a high level of enantioselectivity.

With all these prerequisites in mind, this review intends to summarize the work reported so far (September 2021) in the field of organocatalyzed nucleophilic dearomatization reactions of azaarenium salts (i.e., isoquinolinium, quinolinium, pyridinium and acridinium salts) giving access to corresponding enantioenriched dihydroazaarenes. Publications will be classified according to the organocatalytic mode of activation employed for the dearomatization reaction. Moreover, special attention will be paid to the specific advantages and drawbacks of the modes of activation with respect to specific substrates. Further transformations of dihydroazaarenes allowing the introduction of chemical diversity will also be underlined.

2. Anion-Binding Catalysis

2.1. Activation Mode of Azaarenium Salts in Anion-Binding Catalysis

In organocatalysis, H-bonding donor catalysts (thioureas, squaramides . . .) are better known for their ability to activate neutral electrophiles (Figure 2a) [33,40]. As mentioned earlier, the dearomatization reaction of azaarenes generally requires an activation step namely the formation of an azaarenium flanked by an anion (chloride or bromide in most of the cases) resulting from the reaction of azaarenes with acyl halide derivatives (in situ protocols) or with alkyl halides (preformed ion pair). The ion pair thus formed, allows H-bonding donor catalysts to complex the anion of the substrate thereby forming a well-organized supramolecular chiral entity responsible for the high level of enantioselectivity generally observed through the so-called “anion binding” strategy (Figure 2b). Moreover, even if simple H-bonding donor catalysts provided a high level of enantioselectivity, bifunctional organocatalysts were developed in order to tackle the regioselectivity issue associated with the nucleophilic dearomatization of azaarenium salts. Thus, in addition, to bind the counter ion of the azaarenium salts, these bifunctional catalysts can either (1) guide the nucleophilic partner to a specific electrophilic center of the azaarenium salt thanks to extra H-bonding interactions (Figure 2c) or (2) block one of the electrophilic positions of the azaarenium salts through a first addition thus allowing the second addition of the nucleophile in a highly regioselective fashion (Figure 2d).

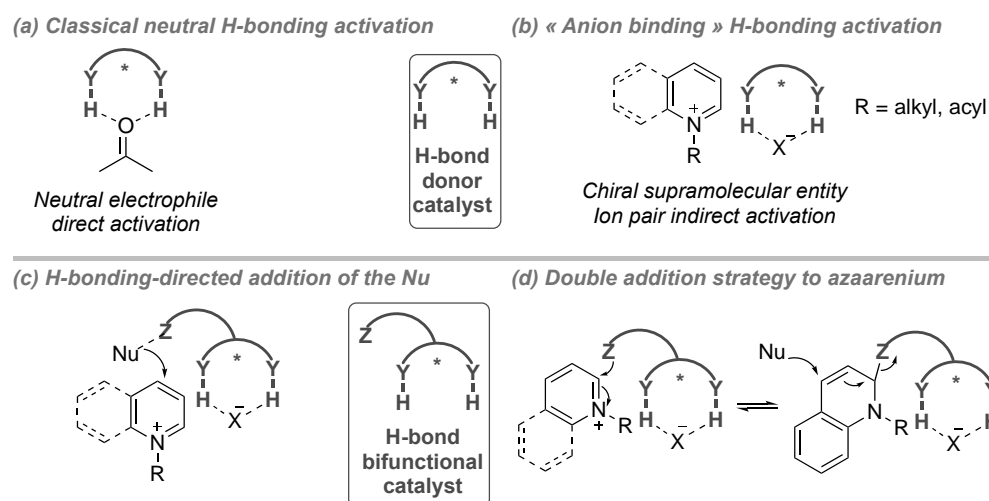
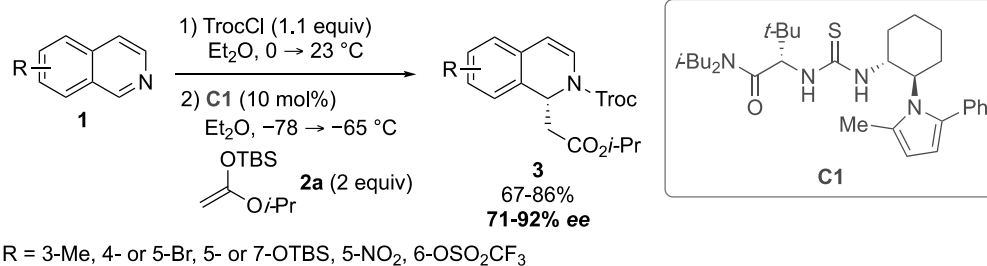


Figure 2. H-bonding catalysis in action.

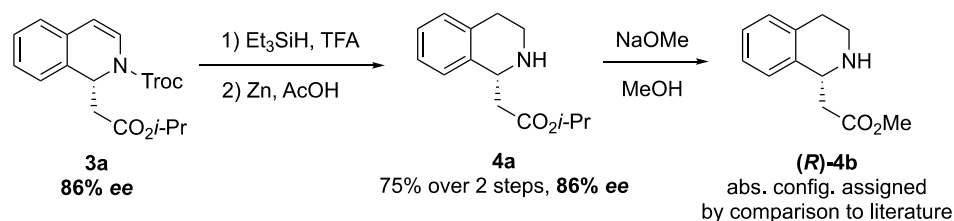
2.2. Isoquinolinium Salts

Pioneering work in anion-binding catalysis applied to the nucleophilic dearomatization of azaarenes was published by Jacobsen et al. concerning a Reissert-type addition of silyl ketene acetal **2a** on isoquinolinium salts formed in situ by reaction between isoquinoline **1** and acyl or carboxyalkyl chloride (Scheme 1) [41]. The optimization of the reaction conditions showed that the Troc moiety on the isoquinolinium salt as well as thiourea catalyst **C1** were necessary to achieve high level of enantioselectivity. With these conditions, a small array of dihydroisoquinolines **3** (8 examples) were then synthesized in acceptable to very good yields (67–86%) and up to 92% *ee* (60–92% *ee*) (Scheme 1a). The synthetic utility of enantioenriched dihydroisoquinoline **3a** was demonstrated by accessing unprotected tetrahydroisoquinoline **4a** via the reduction of the enamide followed by cleavage of the Troc moiety without any racemization. The absolute configuration was assigned by comparing the optical rotation of transesterification product (*R*)-**4b** with literature data (Scheme 1b).

(a) Scope of the reaction



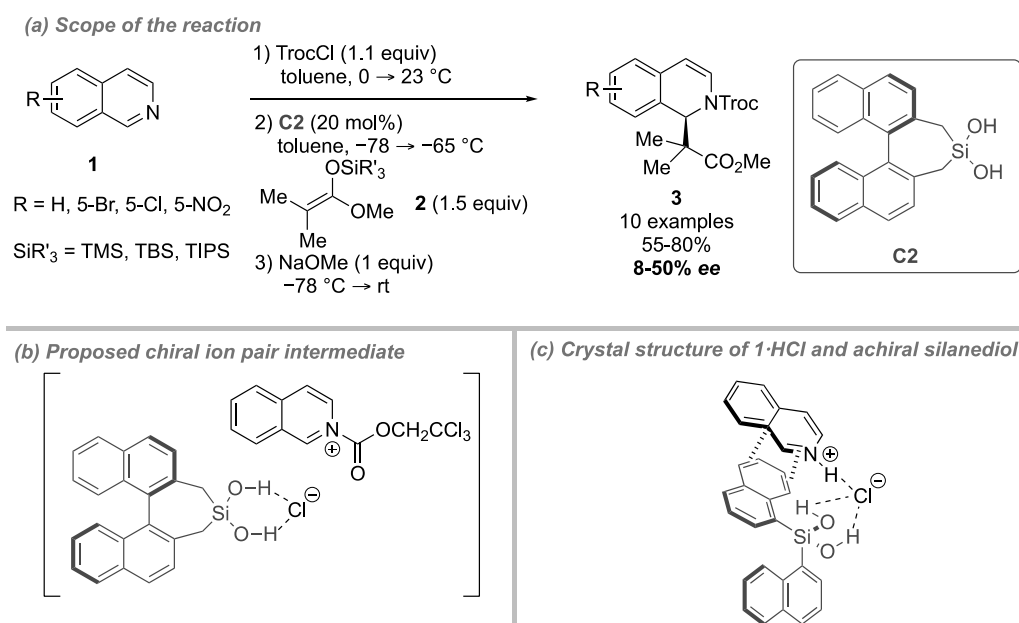
(b) Synthetic transformation



Scheme 1. Reissert-type addition of silyl ketene acetal **2a** catalyzed by chiral thiourea **C1**.

Following this achievement, Mattson et al. developed, in 2013, a similar Reissert-type addition catalyzed with chiral silanediol **C2** (Scheme 2) [42]. Although silanediols have been used as H-bonding donor catalysts in the past [43], this was the first report of silanediols as anion binding catalysts as well as the first synthesis of enantiopure silanediol

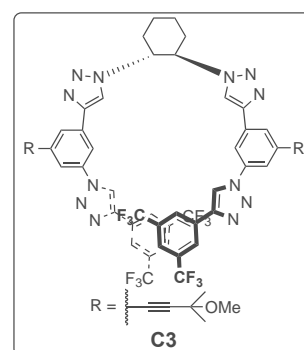
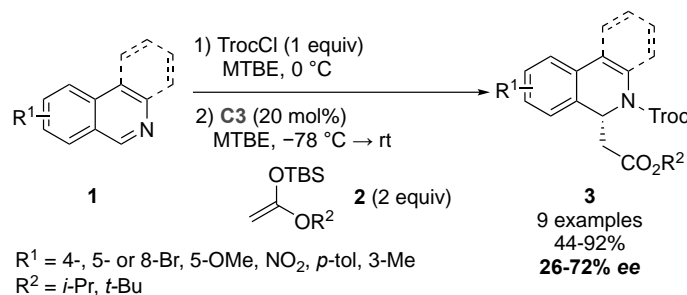
C2 with axial chirality. This catalyst proved to be able to promote the enantioselective addition of silyl ketene acetals **2** to isoquinolinium salts, leading to the corresponding dihydroisoquinolines **3** in acceptable to very good yields (55–80%) and low to moderate *ees* (8–50%); bigger silyl groups SiR_3 leading to higher *ees* (TMS: 8% *ee*; TBS: 18% *ee*; TIPS: 28% *ee*) (Scheme 2a). As far as the mechanism of the reaction is concerned, an NMR study demonstrated that silanediols were able to efficiently bind chloride ions (Scheme 2b), which was further evidenced by crystallization of an ion pair between hydrochloride isoquinolinium salt and achiral silanediol (Scheme 2c).



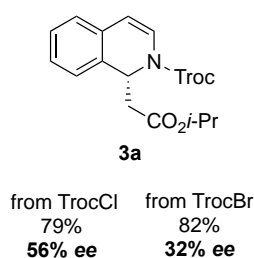
Scheme 2. Reissert-type addition of silyl ketene acetals catalyzed by chiral silanediol **C2**.

Thereafter, in 2016, García Mancheño et al. reported on the dearomatization of isoquinolines during the addition of silyl ketene acetals **2** by means of an original oligotriazole with helicoidal chirality as catalyst (Scheme 3) [44]. An extensive screening showed that an oligotriazole composed of four triazole moieties gave the best results. Among all the tetratriazoles tested, **C3** yielded the best enantioselectivity, leading to dihydroisoquinoline **3a** in 84% yield and an encouraging 38% *ee* despite a strong background reaction (44% yield without catalyst). After further optimization, a range of dihydroisoquinolines **3** were obtained in moderate to excellent yields (44–92%) and *ees* up to 72% (Scheme 3a). It is worth noting that the use of TrocBr instead of TrocCl did not affect the yield of the reaction (Br: 82% yield vs. Cl: 79% yield) although a significant loss of *ee* was observed (Br: 32% *ee* vs Cl: 56% *ee*), suggesting that bromide also binds to **C3** but it does so with a lower efficiency than chloride (Scheme 3b). Finally, kinetic studies evidenced a surprisingly retarded reaction during the first 3 h followed by a marked acceleration of the process. This “delay” was ascribed to the period required for oligotriazole **C3a** to efficiently bind the chloride anion of the isoquinolinium salt (Scheme 3c).

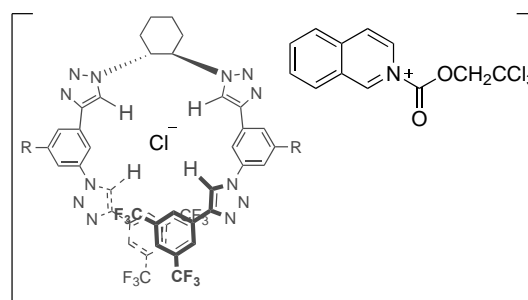
(a) Scope of the reaction



(b) Comparison TrocCl/TrocBr



(c) Proposed active species in the mechanism

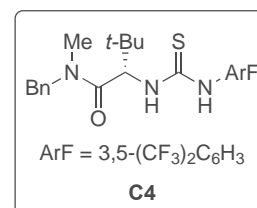
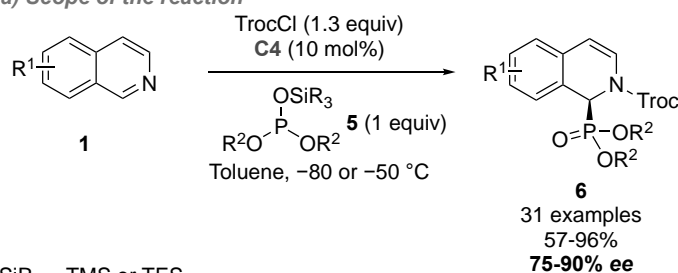


Scheme 3. Reissert-type addition of silyl ketene acetals catalyzed by chiral oligotriazole C3.

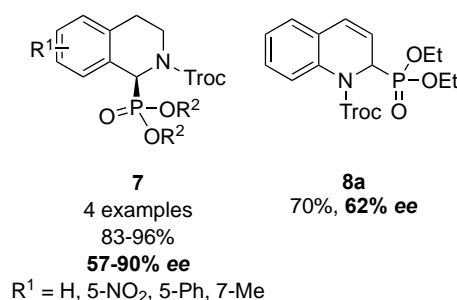
In 2016, Mukherjee et al. expanded the range of possible nucleophiles by reporting the addition of silyl dialkyl phosphites **5** on isoquinolinium salts leading to α -aminophosphoranes (Scheme 4) [45]. Catalyst C4 gave the best results at -80 °C, leading to a wide array of dihydroisoquinolines **6** in acceptable to excellent yields and *ees* generally above 80%, although in some cases a longer reaction time or higher temperature was required to bring the reaction to completion (Scheme 4a). Additionally, this reaction was applicable to dihydroisoquinolines and quinoline, leading respectively to tetrahydroisoquinolines **7** in 77 to 96% isolated yield and up to 90% *ee* and dihydroquinoline **8a** in 70% yield and 62% *ee* (Scheme 4b). The removal of the activating Troc group proved to be challenging. However, Mukherjee's team successfully applied this transformation to *N*-Fmoc-activated quinolinium salt leading to the corresponding *N*-Fmoc-dihydroisoquinoline **7a** (73%, 75% *ee*). Treatment of **7a** by piperidine led to *N*-H tetrahydroisoquinoline **9a** in 91% yield and 62% *ee* (Scheme 4c).

More recently, Lassaletta's team tackled the addition of *N*-*tert*-butyl hydrazones **10** in the dearomatization of isoquinolines **1** (Scheme 5) [46]. It was envisioned that both the catalyst C5 and the hydrazone would be able to bind the chloride anion of the in situ-formed isoquinolinium salt, therefore rigidifying the transition state and leading to high levels of enantioselectivity. This working hypothesis was supported by computational studies of non-covalent interactions and eventually allowed to determine the lowest-energy transition structure leading to the major enantiomer. The optimized conditions yielded the corresponding dihydroisoquinolines **11** in acceptable to good yields, complete diastereoselectivity towards the *anti*-product and excellent *ees* (generally above 90%) (Scheme 5a). However, this reaction was limited to dihydroisoquinolines, as no reaction was observed with pyridines. Moreover, only chloroformates were tolerated as activating groups, since no other activating group (Cbz, Alloc, Ac, Bn) triggered the reaction. The authors performed various synthetic transformations among which the oxidation of the hydrazone moiety in dihydrophenanthridine **12a** (84% yield, >98:2 *dr*, 94% *ee*) (Scheme 5b). It was also evidenced that the hydrazone could be transformed to the corresponding ketone **13a** without any racemization via oxidation of the intermediate imine (70% yield, 94% *ee*).

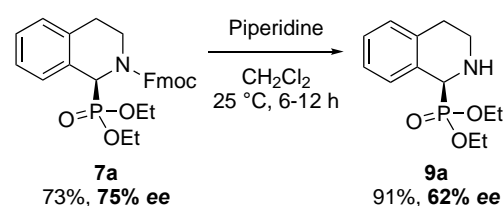
(a) Scope of the reaction

SiR₃ = TMS or TESR¹ = 3-Br, 3-Ph, 3-C≡CPh, 4-Br, 5-NO₂, 5-Br, 6-MeO, 6-Me, 7-Me...R² = Me, Et, *n*-Pr, *i*-Pr

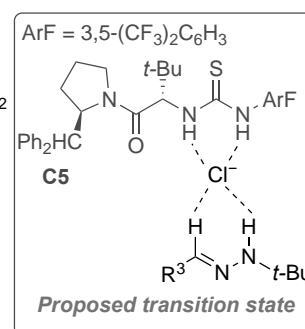
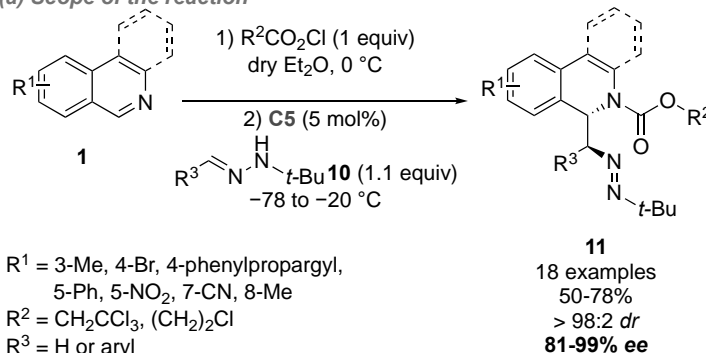
(b) Application to azaarenes 7 and 8



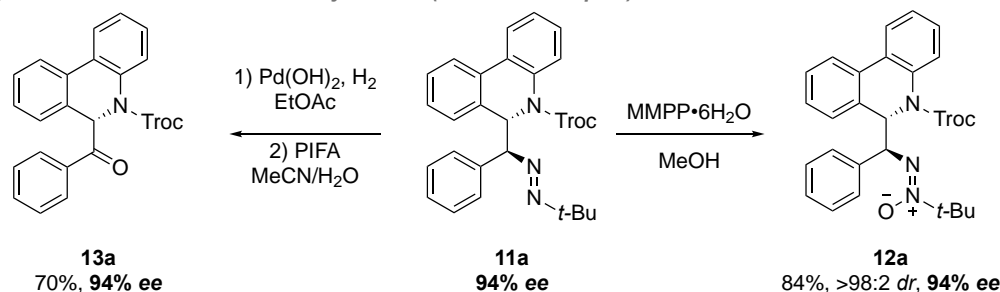
(c) FmocCl as activating group

**Scheme 4.** Addition of silyl phosphites 6 to isoquinolinium salts catalyzed by chiral thiourea C4.

(a) Scope of the reaction

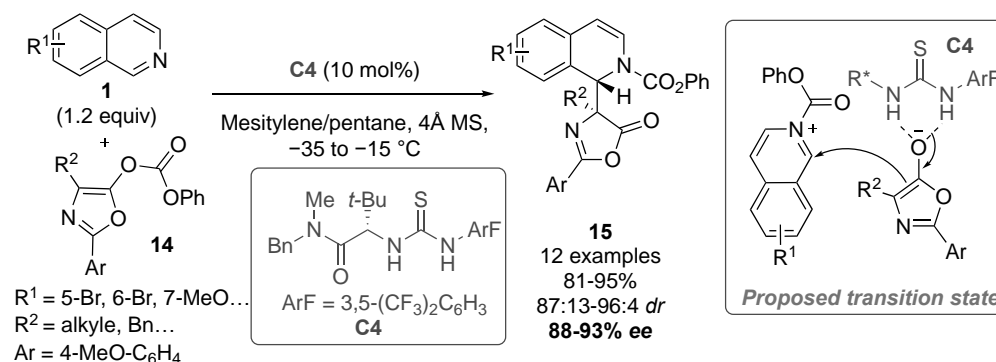


(b) Post-fonctionnalization of the hydrazone (selected examples)

**Scheme 5.** Addition of hydrazones to isoquinolinium salts catalyzed by chiral thiourea C5.

As part of an effort to develop new dual-catalysis approaches in organocatalysis, Seidel's group reported on the enantioselective addition of azlactones **14** to isoquinolines **1** (Scheme 6) [47]. Unlike previous reactions in this chapter, there was no need for an external activating group such as TrocCl since the carboxyalkyl moiety of the azlactone was able to interact with isoquinoline **1** to form the corresponding isoquinolinium salt *in situ*. The enantioselective addition of the enolate (complexed by catalyst **C4**) to the isoquinolinium

salt at the C1 position led to the corresponding dihydroisoquinolines **15**. During the optimization, it was found that the strong background reaction (95% yield at $-10\text{ }^{\circ}\text{C}$ for 3 h in mesitylene) could be avoided both by lowering the temperature and using more apolar solvents. These optimized conditions were then applied to a variety of isoquinolines **1** and azlactones **14**, yielding differently substituted dihydroisoquinolines **15** in excellent yields (81–95%), diastereoselectivities (87:13 to 96:4 *dr*) and high enantioselectivities (88–93% *ee*).



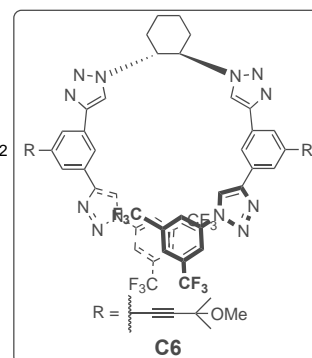
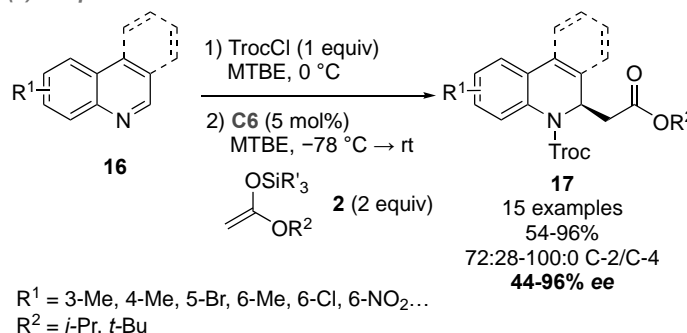
Scheme 6. Addition of azlactones to isoquinolinium salts catalyzed by chiral thiourea **C4**.

2.3. Quinolinium Salts

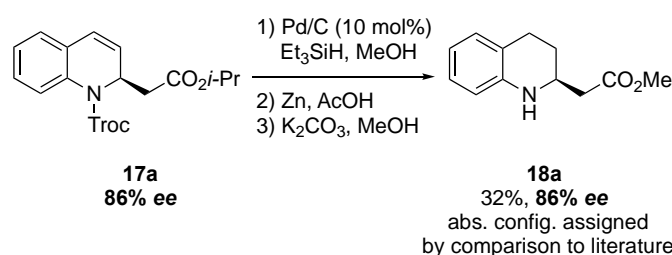
In 2014, García Mancheño et al. reported on the dearomatization of quinolines **16** via Reissert-type addition of silyl ketene acetals **2** catalyzed by a chiral oligotriazole **C6** (Scheme 7) [48]. The reaction occurred in a one-pot sequence involving (1) the activation of the quinoline into a quinolinium salt and (2) addition of the silyl ketene acetals **2** onto the quinolinium salt. During the optimization of the reaction conditions, bistriazole **C6** (Scheme 7c) was tested but provided very low selectivity (91%; 18% *ee*), therefore underlining the need for helicoidal chirality to ensure an efficient chirality transfer. Tetra-triazole **C6** was therefore chosen as the best catalyst, and an array of dihydroquinolines **17** (15 examples) were synthesized on average to excellent yields (67–86%) and up to 92% *ee* (60–92% *ee*) (Scheme 7a). In order to demonstrate the synthetic utility of the so-obtained enantioenriched dihydroquinolines **17**, substrate **17a** was reduced into the corresponding tetrahydroisoquinoline **18a** without any racemization (Scheme 7b). Absolute configuration was assigned by comparison of the optical rotation with literature data of the unprotected product **18a**. Finally, NMR and circular dichroism studies provided mechanistic insight by highlighting the accommodation of the chloride anion inside the chiral cavity of catalyst **C6** through H-bonding interactions.

In 2017, García Mancheño et al. extended this methodology to the addition of silyl dialkyl phosphites **5** on quinolines **16** catalyzed by chiral oligotriazole **C6** (Scheme 8) [49]. The desired dihydroquinolines **8** were obtained in average to good yields (59–95%) and generally very good *ees* (up to 94% *ee*) (Scheme 8a). If the 1,2-dihydroquinolines remained the major regioisomer in all cases (vs 1,4-dihydroquinolines), the authors observed that the presence of residual moisture decreases both yield and regioselectivity. The authors showed that aminophosphorane **8b** (84% *ee*) could undergo further transformations such as the reduction of the dihydroquinoline core to tetrahydroquinoline **19a** (99%, 84% *ee*) or the transesterification of the phosphite (**8a**, 71% over three steps, 84% *ee*) without any observable racemization (Scheme 8b).

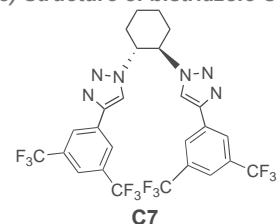
(a) Scope of the reaction



(b) Synthetic transformation



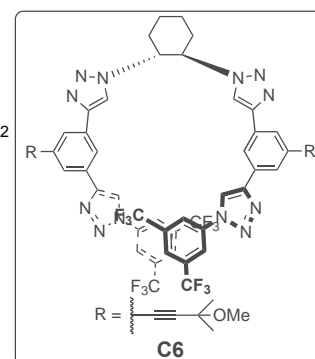
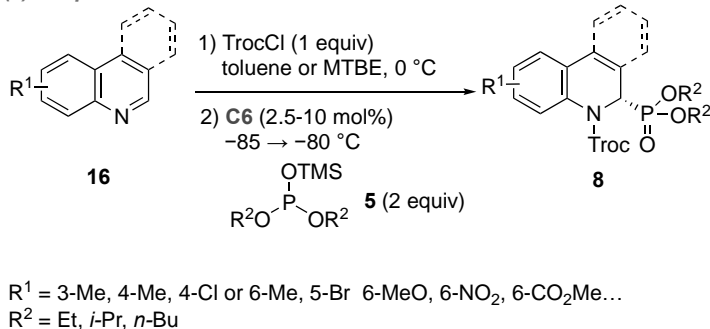
(c) Structure of bistriazole C7



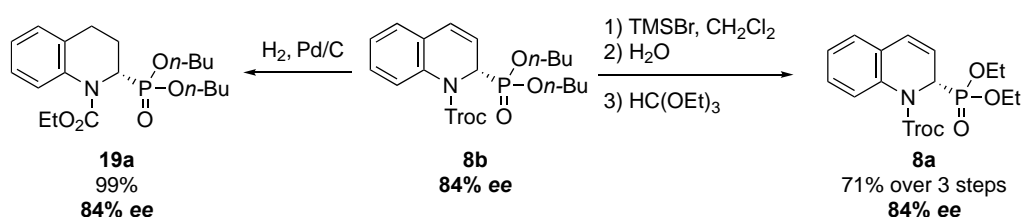
(for $\text{R}^1 = \text{H}$, $\text{R}^2 = i\text{-Pr}$: 91%; **18** ee)

Scheme 7. Addition of ketene silyl acetals **2** to quinolinium salts catalyzed by chiral oligotriazole **C6**.

(a) Scope of the reaction

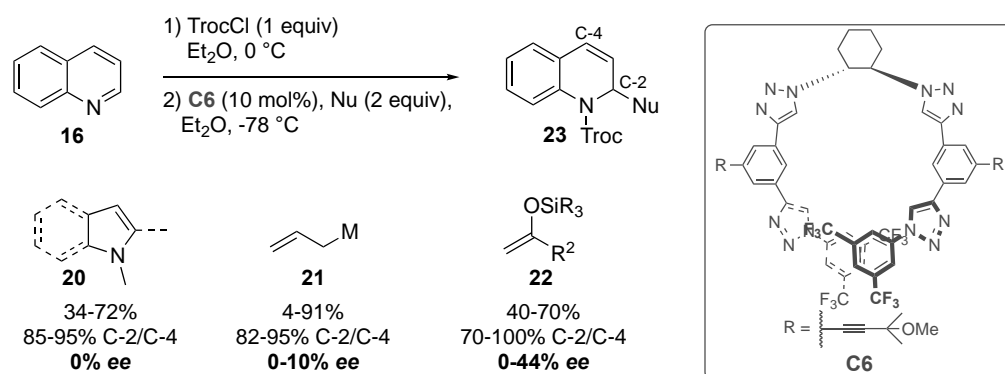


(b) Synthetic transformation



Scheme 8. Addition of silyl phosphites **5** to quinolinium salts catalyzed by chiral oligotriazole **C6**.

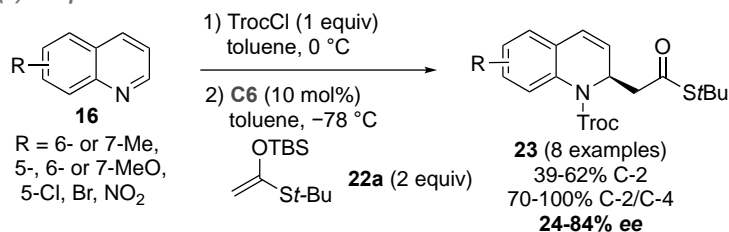
In order to further expand the scope of this organocatalytic dearomatization of quinolines **16**, García Mancheño et al. tested the conditions they had previously developed on other nucleophiles (Scheme 9) [50]. Among them, electron-rich heterocycles **20** and metal allyl reagents **21** led to the corresponding 1,2-dihydroquinolines **23** as the major product with almost no enantioselectivity by using **C6** as organocatalyst. On the other hand, encouraging results were obtained with silyl enol derivatives, and especially with silyl ketene thioacetal **22** ($\text{R}^2 = \text{St-Bu}$, 50% yield, 70% C-2/C-4, 44% ee), which was therefore subjected to further optimization.



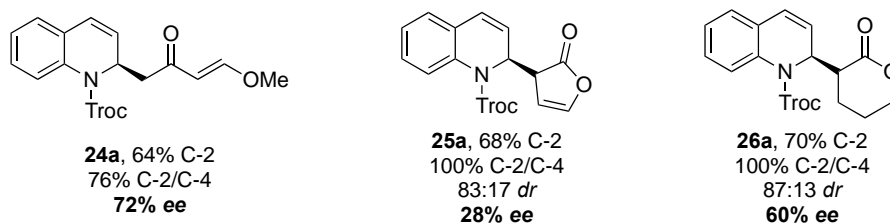
Scheme 9. Nucleophiles screening in the dearomatization of quinolinium salts catalyzed by chiral oligotriazole **C6**.

The optimization of the reaction with silyl ketene thioacetal **22** provided a range of 1,2-dihydroquinolines **23** with 39 to 62% yield, good to complete regioselectivity and *ees* up to 84% (Scheme 10a). Other silyl-based nucleophiles were then tested under these conditions to provide the corresponding 1,2-dihydroquinolines **24–26** (Scheme 10b). The best *ee* was obtained with Danishefsky's diene, yielding 1,2-dihydroquinoline **24a** with 64% yield and 72% *ee*. The synthetic utility of the thioesters **23a** was shown through a four-step synthesis furnishing the corresponding N-tosyl tetrahydroquinoline **27a** without any racemization (Scheme 10c).

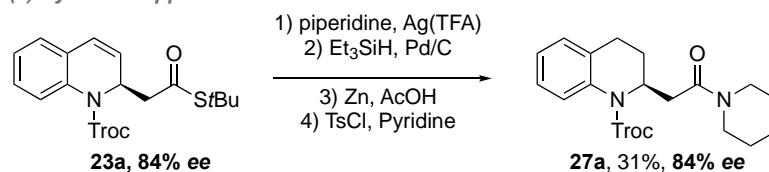
(a) Scope of the reaction



(b) Silyl-based nucleophile screening



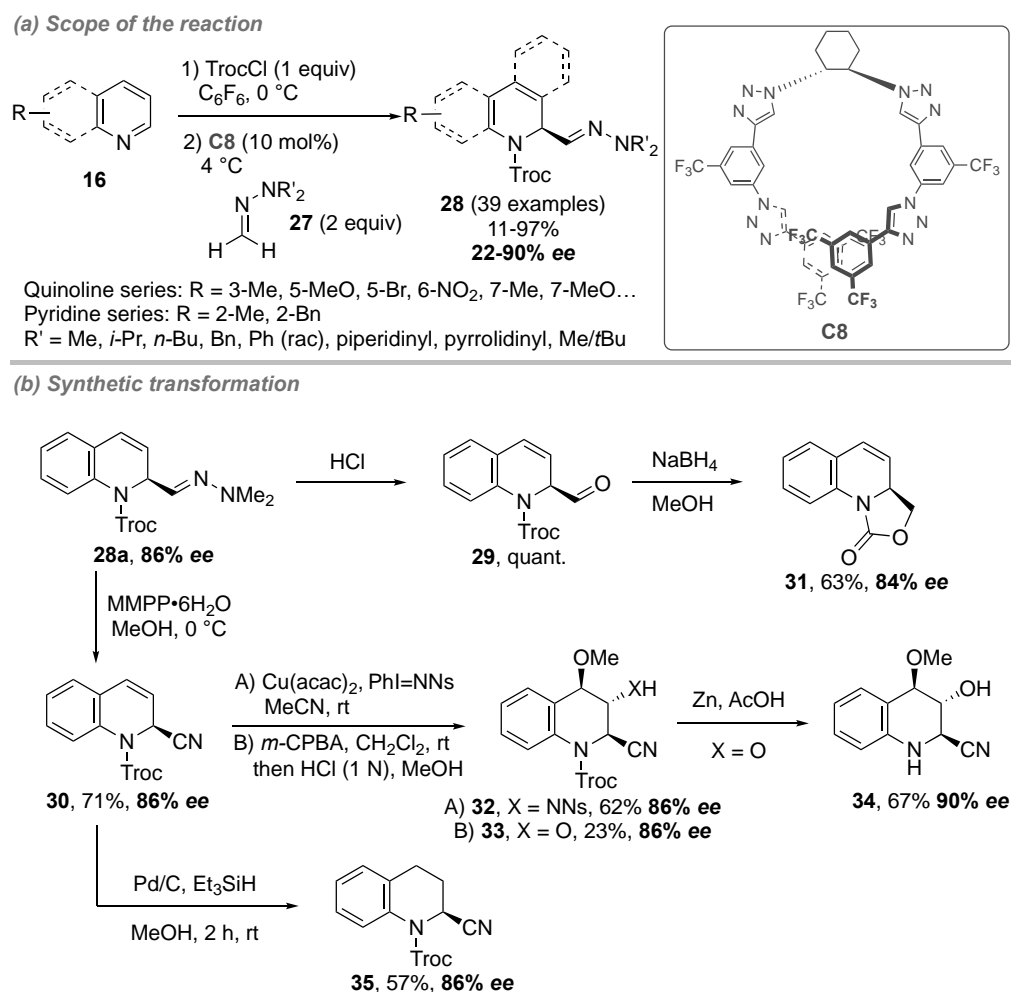
(c) Synthetic application



Scheme 10. Addition of silyl ketene thioacetal **22a** to quinolinium salts catalyzed by chiral oligotriazole **C6**.

More recently, García Mancheño et al. reported on the addition of formaldehyde-derived hydrazones **27** to quinolines **16** catalyzed by chiral oligotriazole **C8** (Scheme 11) [51]. During the optimization, catalyst **C8** proved to be superior to tetratriazole **C6** and it was hypothesized that the anion-binding affinity could be enhanced through H-bonding between the CF_3 group of **C8** and carbonyl hydrogen of the hydrazone. A large range of dihydroquinolines **28** (39 examples) were obtained in low to excellent yields (11–97%)

and generally very good *ees* (up to 90% *ee*) (Scheme 11a). It is worthy of note that the reaction was also applied to a couple of pyridine derivatives (18–30%, 70–80% *ee*), albeit less efficiently. Dihydroquinoline **28a** could be transformed either to the corresponding aldehyde **29** or carbonitrile derivatives **30**, which could, in turn, be subjected to further modifications to afford compounds **31–35** without any racemization (Scheme 11b). Finally, DFT calculations allowed the authors to propose a lowest-energy transition state that thanks to the H-bonding network and preorientation of the nucleophile provides the desired products with (S)-absolute configuration.

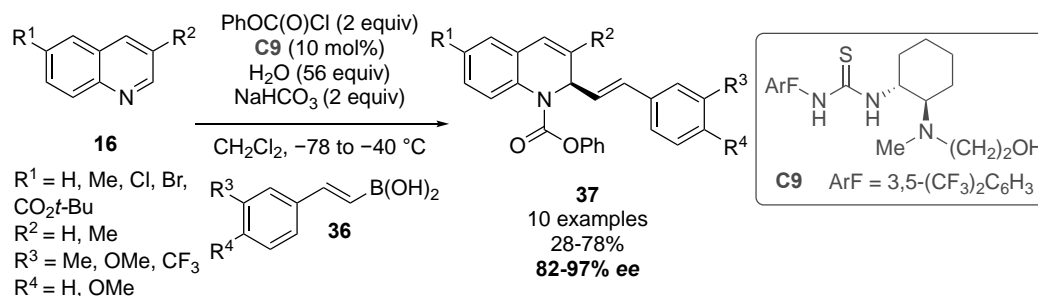


Scheme 11. Addition of N,N-hydrazones **27** to quinolinium salts catalyzed by chiral oligotriazole **C8**.

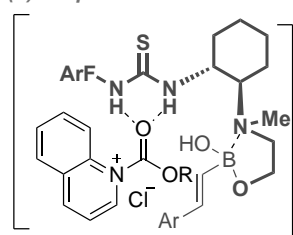
Takemoto et al. described a Petasis-type addition of vinyl boronic acids **36** to quinolines **16** using a dual-catalysis approach but making use of a different type of anion-binding activation strategy (Scheme 12) [52]. During the optimization, the addition of H₂O and NaHCO₃ in the reaction was beneficial to the reaction. Water seemingly enhanced the enantioselectivity by assisting the regeneration of the catalyst, while with NaHCO₃, an increase of the yield was observed, which was attributed to the trapping of the boronic acid formed during the reaction. With the optimized conditions in hand, an array of 1,2-dihydroquinolines **37** were synthesized with complete regioselectivity, and yields ranging from 28 to 78% as well as very good to excellent *ees* (82–97% *ee*) (Scheme 12a). In this reaction, bifunctional catalyst **C9** is composed of a thiourea moiety that binds the intermediate N-acyl quinolinium while the 1,2-aminoalcohol part complexes the boronic acid, bringing the substrates in close proximity to obtain 1,2-dihydroquinoline **37** (Scheme 12b). In order to showcase the use of these substrates, (+)-Galipinine **38a** was synthesized from dihydro-

quinoline **37a**, which also enabled the authors to determine the absolute configuration of the obtained products by comparison to the literature (Scheme 12c).

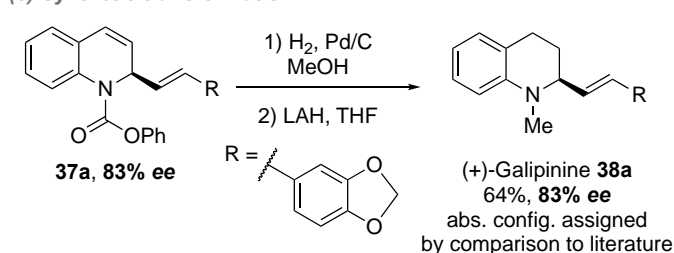
(a) Scope of the reaction



(b) Proposed TS



(c) Synthetic transformation



Scheme 12. Addition of boronic acids **36** to quinolinium salts catalyzed by bifunctional catalyst **C9**.

2.4. Pyridinium Salts

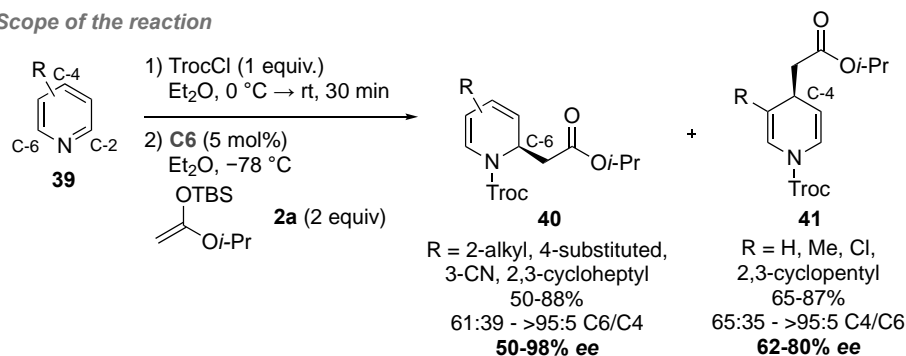
As previously seen, the dearomatization of azaarenium salts gave rise to highly functionalized N-heterocycles but, dearomatization of pyridines poses additional challenges. Firstly, the complete loss of aromaticity during the reaction (unlike quinolines and isoquinolines) heightens the energetic cost of the reaction, rendering pyridines less reactive than their N-heteroarenes counterparts. Moreover, the three electrophilic positions on the pyridinium nucleus (C2, C4 et C6) make the control of the regioselectivity very challenging.

In 2015, García Mancheño's team was the first to report the enantioselective organocatalytic dearomatization of pyridinium salts using oligotriazole catalyst **C6** (Scheme 13) [53]. The authors successfully transposed their previous work describing the “anion-binding” catalysis-mediated addition of silyl ketene acetals **2** on the in situ-formed quinolinium to pyridinium counterparts. After careful optimization, the scope of the reaction was studied on a variety of pyridines **39**, leading to the corresponding dihydropyridines **40–41** in 50 to 87% yield and up to 98% ee (Scheme 13a). However, in this reaction, regioselectivity was highly dependent upon the substitution of the pyridine on positions C2, C3 and/or C4. As a general trend, substitution of the pyridine on position C2 or C4 led to the corresponding 1,6-dihydropyridines **40** (94:6 to 100:0 C6/C4) whereas substitution on position C-3 yields 1,4-dihydropyridines **41** as the major product (95:5 to 0:100 C6/C4 except for $\text{R} = 3\text{-CN}$, 61:39 C6/C4), as it is also the case with the unsubstituted pyridine (35:65 C6/C4). The authors further modified dihydropyridines **40a** and **41a** by reduction to the corresponding tetrahydropyridines **43a** and **42a** respectively and removing the Troc activating group without observing any racemization (Scheme 13b).

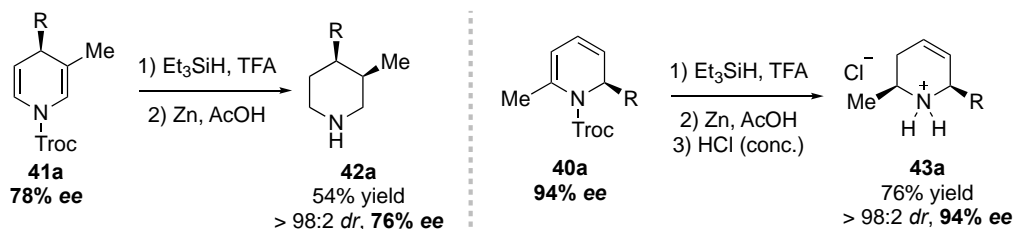
The conditions, previously reported by the same group for the addition of dialkyl phosphites **5** to quinolinium salts (see Scheme 8), were also extended to pyridinium salts (Scheme 14) [49]. The desired dihydropyridines **44** were generally obtained in lower ees (52–78% ee) (Scheme 14a). Complete control of the regioselectivity could be achieved in most cases, but low noticeable amounts of 1,4-dihydropyridines were observed with 3-picoline and pyridine (C6/C4: 93:7 and 92:8 respectively). The dearomatization was also performed with CbzCl as an activating agent albeit less successfully (**44a**, 79% yield, 30% ee), followed by reduction and Cbz-removal of the intermediate dihydropyridine **44a**, thus

yielding pipecolic phosphonic acid **45** in 50% over 2 steps, whose absolute configuration has been assigned based on the literature data (Scheme 14b).

(a) Scope of the reaction

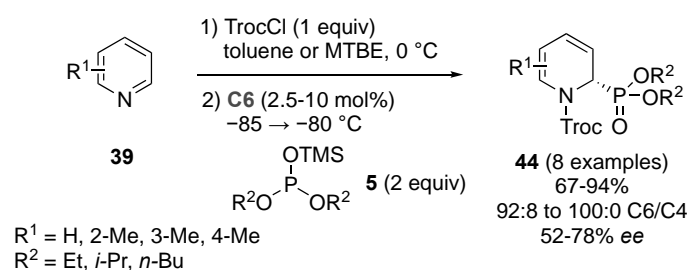


(b) Synthetic transformation (R = CH₂CO₂i-Pr)

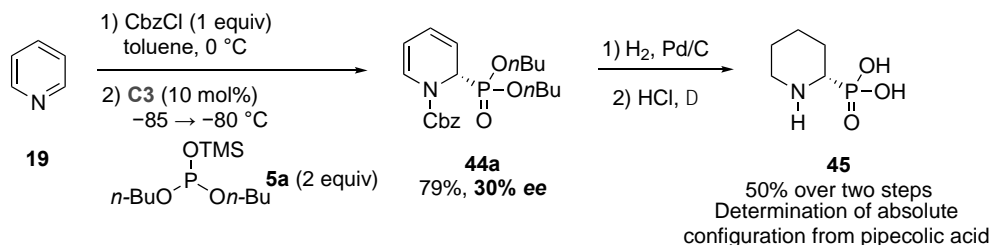


Scheme 13. Addition of ketene silyl acetal **2a** to pyridinium salts catalyzed by chiral oligotriazole **C6**.

(a) Scope of the reaction



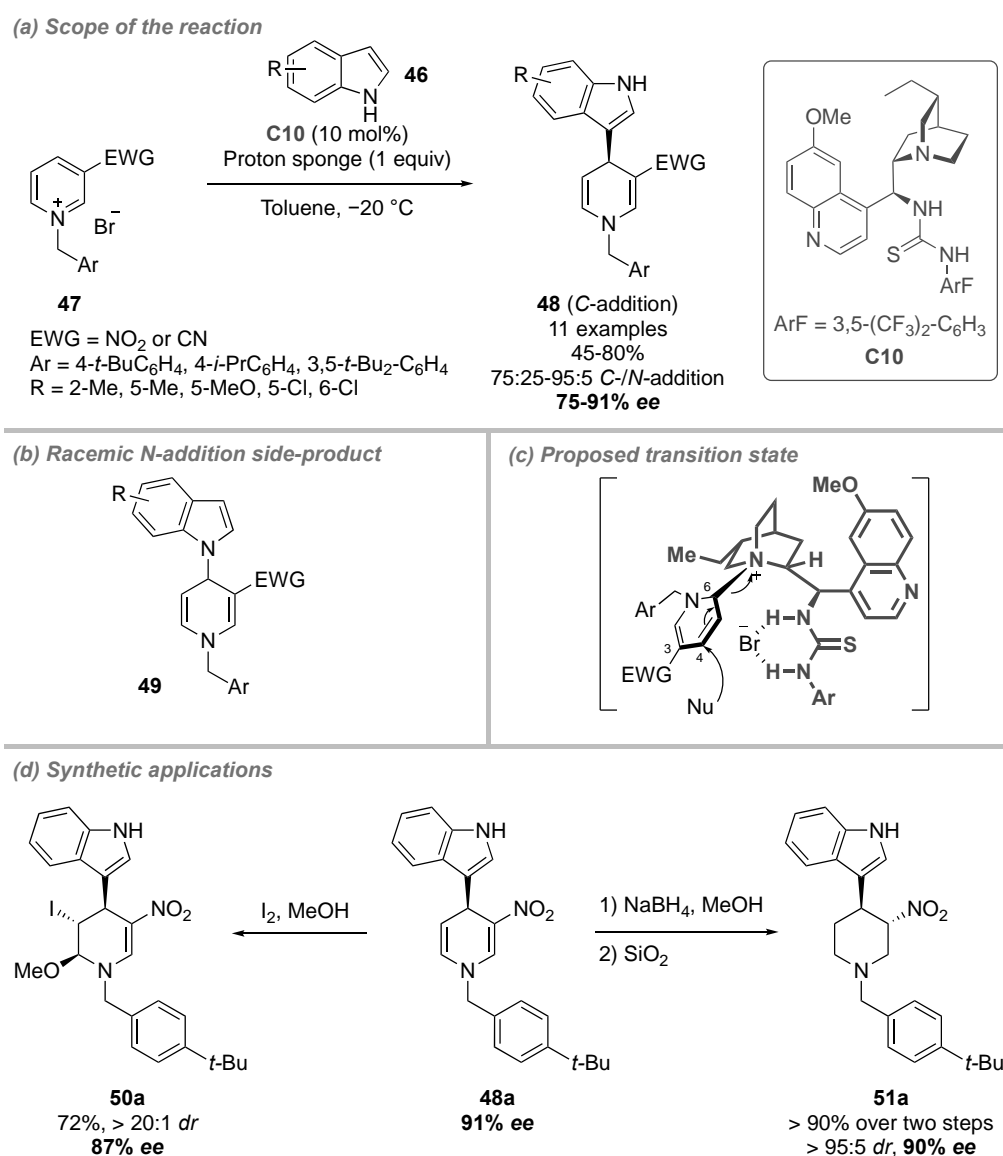
(b) Synthetic transformation



Scheme 14. Addition of silyl phosphites **5** to pyridines derivatives catalyzed by chiral oligotriazole **C6**.

After García Mancheño's pioneering work on the organocatalytic dearomatization of pyridinium salts, Bernardi et al. described the regio- and enantioselective addition of indoles **46** to N-alkyl pyridinium salts **47** (substituted by an electron withdrawing group on C3 position) catalyzed by chiral thiourea **C10** (Scheme 15) [54]. It is worthy to note that this is the only reaction to date that involves both anion-binding catalysis and N-alkyl azaarenium salts, affording highly regioselective addition at the C4 position. However, the optimization proved to be tricky: a base had to be added to neutralize the

HBr formed in the reaction, but consequently, an undesired racemic product from the base-promoted N-addition of the indole **46** was observed (71:29 C/N ratio) (Scheme 15b). This problem was overcome by adding the base with a syringe pump over 10 h (75:25 to >95:5 C/N ratio). Moreover, a sterically hindered benzyl group was necessary to reach good levels of enantioselection. Under these optimized conditions, 1,4-dihydropyridines **48** were obtained with complete regioselectivity in moderate to very good yields (45–80%) and *ees* up to 91% (Scheme 15a). Interestingly, 3-nitropyridinium salts **47** (EWG = NO₂) led to better results (70–80%, 90–91% *ee* for the corresponding product **48**) compared to 3-cyanopyridinium salts **47** (EWG = CN) (45–55% and 80–89% *ee* with 15 mol% **C10** at room temperature for the corresponding product **48**). The authors showed the synthetic potential of the resulting 1,4-dihydropyridine **48a** by performing (1) an iodoetherification to provide **50a** (72%, >95:5 *dr*, 87% *ee*) and (2) a reduction furnishing the tetrahydropyridine **51a** (>90%, >95:5 *dr*, 90% *ee*) (Scheme 15d). An NMR study led to a proposal for the transition state where the quinuclidine moiety of thiourea **C10** adds to the C6 position of the pyridinium salt to form an aminal thus avoiding the addition of the nucleophile at this position. Accordingly, the indole addition occurs regioselectively at the C4 position through an S_N2' type-mechanism (Scheme 15c).

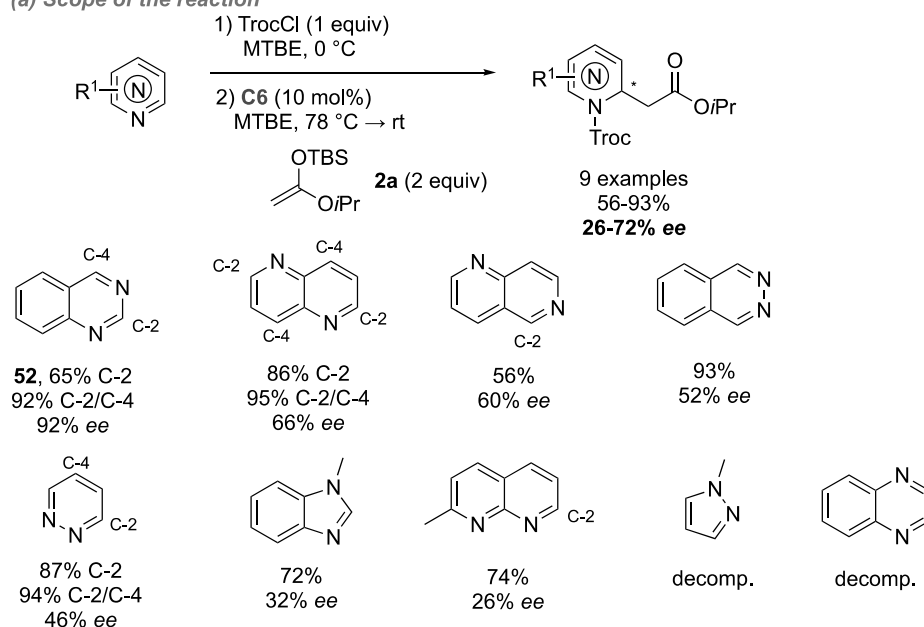


Scheme 15. Addition of indoles to *N*-alkylpyridinium salts **47** catalyzed by chiral thiourea **C10**.

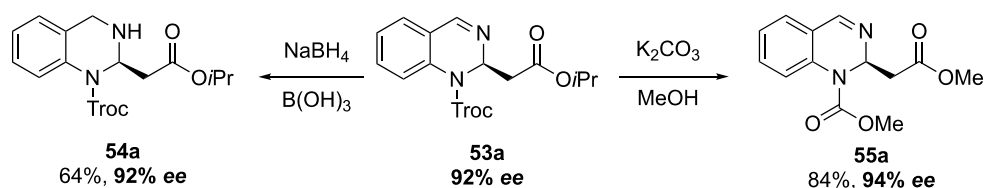
2.5. Others

Up to date, the topic of diazaarene dearomatization has remained elusive in the literature and only one paper comes from García Mancheño's team who reported the addition silyl ketene acetal **2a** on a range of diazaarenes catalyzed by chiral triazole **C6** (Scheme 16) [55]. Optimization of the reaction for quinazoline **52** led to the corresponding product with an excellent 92% *ee* (Scheme 16a). However, attempts to transpose the reaction to other azaarenes (naphthyridine, phthalazine, pyridazine, naphthyridine . . .) resulted in a steep loss of enantioselectivity at best and, at worst, complete decomposition of the product (pyrazole, quinoxaline). The authors successfully performed further synthetic transformations from quinazoline adduct **53a**, such as sodium borohydride-mediated reduction of the pyrimidine cycle (**54a**, 64%, 88% *ee*) or transesterification of the Troc moiety to a methylcarbonate (**55a**, 84%, 94% *ee*); both reactions were conducted without erosion of the enantioselectivity (Scheme 16b).

(a) Scope of the reaction



(b) Synthetic transformations

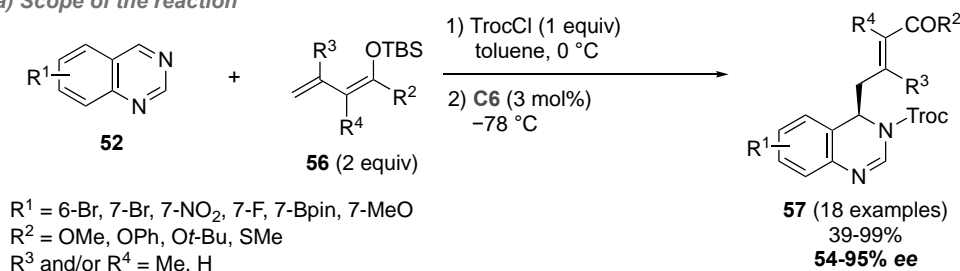


Scheme 16. Addition of silyl ketene acetal **2a** to diazaarenium salts by chiral oligotriazole **C6**.

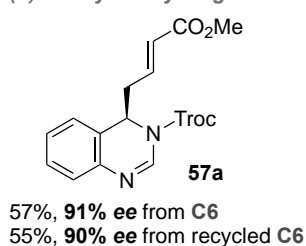
Very recently, the group of García-Mancheño extended the dearomatization of quinazoline derivatives **52** by implementing a vinylogous-Mukaiyama type addition of silyl dienol ethers **56** (Scheme 17) [56]. In the presence of only 3 mol% of catalyst **C6**, a highly regioselective C4-addition (>25:1) occurred providing several dearomatized adducts **57** in modest to high isolated yields (39–99%) and fair to excellent level of enantioselectivity (54–95% *ee*) (Scheme 17a). The aromatic ring of the quinazoline can be substituted by a wide array of substituents (F, NO₂, Br, Me, Bpin . . .) at the 5-, 6- or 7-position. It is worthy of note that the absolute configuration was assigned thanks to X-ray crystallographic analysis. Regarding the substitution of the silyl dienol ethers **56**, several R² groups were evaluated (OMe, Ot-Bu, OPh, SMe) showing that except for the SMe substituent, excellent levels of enantioselectivity were obtained (R¹ = H, 92% *ee* vs 64% *ee* respectively). Interestingly,

catalyst **C6** can be recovered from the reaction mixture in 90% yield and re-used without any loss in both yield and *ee* (Scheme 17b). This strategy has also been successfully applied to quinoline and pyridine derivatives provided that the conditions were slightly modified (10 mol% of **C8** in Et₂O:C₆F₆ (3:1) at −30 °C or in C₆F₆ at 6 °C respectively) (Scheme 17c). Whereas quinoline derivatives afforded the corresponding dihydroazaarenes **58** in high yields and enantiomeric excesses (57–81%, 64–82% *ee*), the only example reported in the pyridine series yielded lower yield and *ee* (**59a**, 46%, 40% *ee*). Finally, dihydroquinazoline **57a** has been derivatized into chiral lactam **61** by N-deprotection of the Troc group followed by selective hydrogenation of the double bond of **60a** in a modest 47% yield over two steps but without any racemization (Scheme 17d).

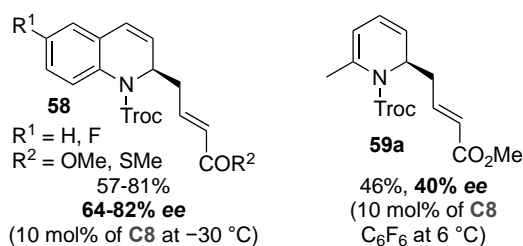
(a) Scope of the reaction



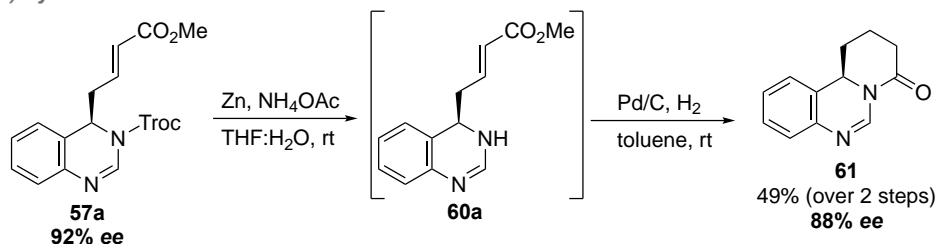
(b) Catalyst recycling



(c) Other azaarenes



(d) Synthetic transformations



Scheme 17. Vinylogous-Mukaiyama-type addition of silyl dienol ethers derivatives **56** to (dia)zaarenium salts by chiral oligotriazole **C6** or **C8**.

3. Aminocatalysis

3.1. Activation Mode of Azaarenium Salts in Aminocatalysis

Since the advent of organocatalysis in the early 2000s, aminocatalysis (or catalysis by primary or secondary amines) has been defined as the method of choice for the activation at the α -CH or β -CH position of carbonyl compounds by the formation of an iminium or an enamine species respectively [57]. In the next paragraphs, we will focus on the nucleophilic addition of carbonyl compounds mostly aldehydes to azaarenium salts catalyzed by chiral primary or secondary amines derived from proline or *Cinchona* alkaloids through the formation of iminium/enamine intermediates (Figure 3). Generally speaking, this mode of activation provides excellent regioselectivity for the addition (1,4- vs. 1,2-addition) depending on the azaarenium salt involved, and modest to high diastereoselectivity and excellent enantioselectivity. Nevertheless, despite these promising features, several drawbacks remain to be addressed. The first one deals with the low electrophilicity of the azaarenium salt especially for *N*-alkyl pyridinium salts thus requiring

the introduction of an electron-withdrawing substituent generally at the C3 position of the ring. Moreover, addition products are sometimes difficult to purify due to their poor stability thus, requiring an additional chemical transformation prior to the isolation of the product. The most widespread one is the carbonyl reduction into the corresponding alcohol but the Wittig reaction was also reported to be efficient. Finally, the last step of the catalytic cycle, namely the hydrolysis of the iminium intermediate to afford the desired product along with the regeneration of the chiral catalyst, results in the formation of a stoichiometric amount of HX that could be detrimental for the next catalytic cycles. In order to prevent any problems, the addition of an extra achiral Brønsted base, at least, in a stoichiometric amount is mandatory. Considering the aforementioned points, the set-up of optimized conditions for the aldehyde addition to azaarenium under aminocatalytic conditions proves to be challenging as shown below.

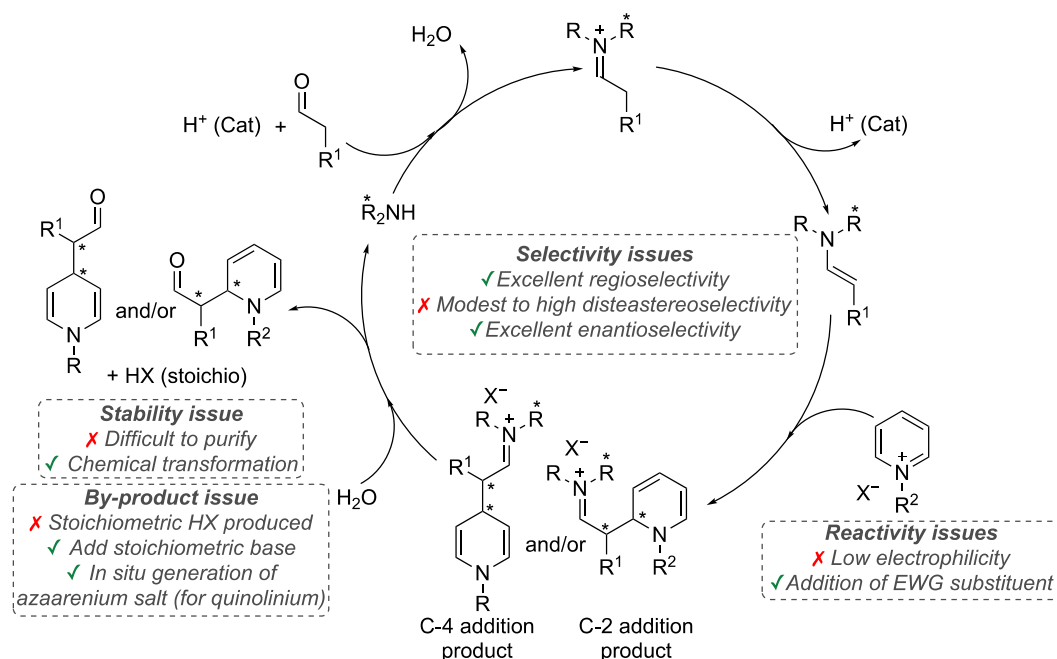


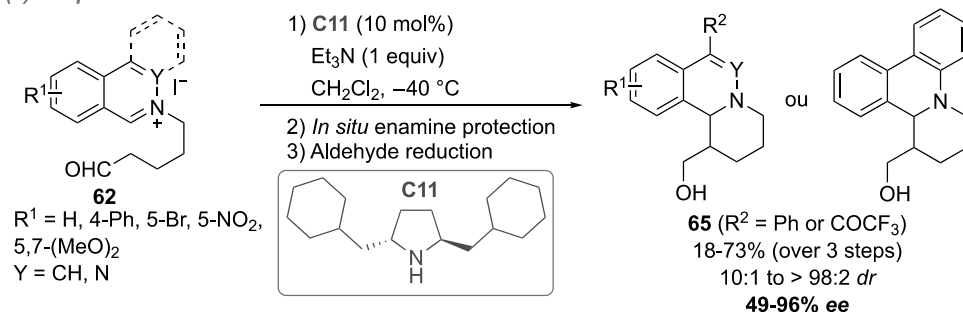
Figure 3. General considerations for enantioselective dearomatization of azaarenium salts by aminocatalysis. * refers to either a stereogenic center or a chiral catalyst.

3.2. Isoquinolinium Salts

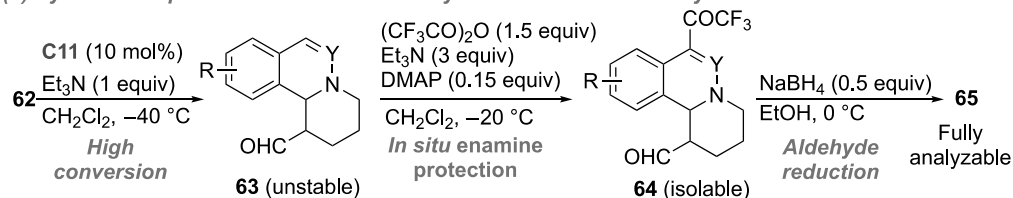
The first report using aminocatalysis for the dearomatization of isoquinolinium salts **62** was published by the group of Jørgensen in 2005 by making use of (2*S*,5*S*)-2,5-dibenzylpyrrolidine **C11** as a catalyst (Scheme 18) [58]. By taking advantage of the presence of an aldehyde on the 2-(5-oxopentyl)isoquinolinium derivative **62**, an enamine intermediate was formed in the presence of the chiral catalyst **C11** and added to the electrophilic carbon of the isoquinolinium moiety. Then, after the ring closure, hydrolysis of the transient iminium ion provided the 1,2-dihydroquinoline derivatives **63**. The generated HX was trapped by external base Et₃N, to allow the catalyst regeneration. 1,2-dihydroquinoline derivatives **63** were obtained in high conversions but revealed to be unstable and, thus, first required the in situ protection of the enamine by a trifluorocetylation reaction catalyzed by DMAP (for compound without substituent at C-4 position) to afford **64** which could be isolated. Finally, the reduction of the aldehyde function of **64** to the corresponding alcohol gave a fully analyzable product **65** (Scheme 18b). Generally speaking, moderate isolated yields (over three steps) below 73% were obtained. Nevertheless, high diastereomeric ratios (15:1 to >98:2) and an excellent level of enantioselectivity (85–96% *ee*) were observed for products **65**. Even phthalazine skeleton (Y = N) was well-tolerated providing dihydrophthalazines **65** with interesting yield, *dr* and *ee* (59%, >98:2, 93% respectively) (Scheme 18a). It

is worthy of note that the presence of electron-donating groups on the aromatic part of the isoquinoline ring ($R^1 = 5,7\text{-(OMe)}_2$) was the main limitation resulting in a drastic drop of the conversion (50%), diastereomeric ratio (10:1) and enantioselectivity (49% *ee*).

(a) Scope of the reaction



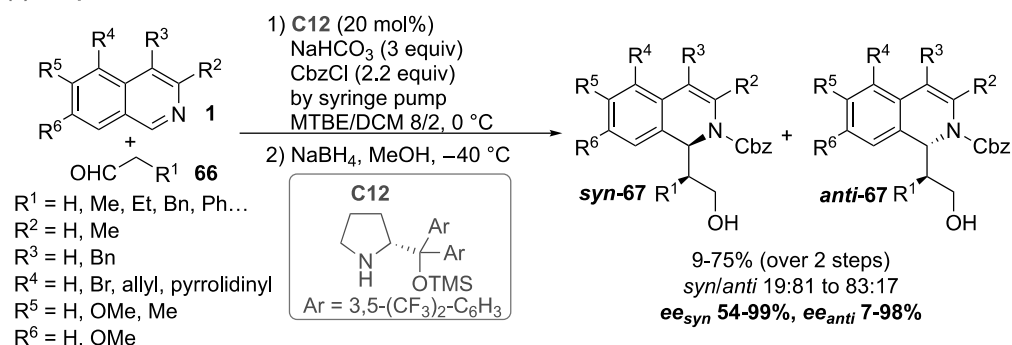
(b) Synthetic sequence to overcome stability issue and to allow analysis



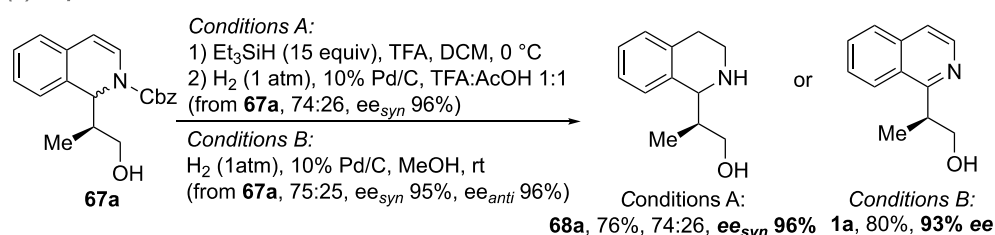
Scheme 18. Diastereo- and enantioselective annulation reaction for the dearomatization of isoquinolinium salts **62** catalyzed by aminocatalyst **C11**.

Several years later, Cozzi et al. reported on an intermolecular addition of aldehydes **66** to in situ-generated isoquinolinium salts in the presence of Hayashi–Jørgensen catalyst **C12** (Scheme 19) [59]. Indeed, the quinolinium salt was generated upon slow addition of CbzCl via a syringe pump to the reaction mixture composed of the isoquinoline **1**, the catalyst **C12** (20 mol%), NaHCO₃ (3 equiv) in TBE/DCM (8/2) (Scheme 19a). It should be noted that MacMillan catalyst **C13** (see Scheme 22 for the structure) failed to promote the reaction due to a lower rate of production of the enamine intermediates compared to Hayashi–Jørgensen catalyst **C12**. Thus, by reacting several aliphatic aldehydes **66** with C3, C4, C5, C6 or C7-substituted isoquinoline derivatives **1**, dihydroisoquinolines **67** were isolated, provided that the aldehyde intermediate was reduced into the corresponding alcohol (NaBH₄, MeOH), as a mixture of *syn/anti* diastereomers (19:81 to 87:13; in most cases the diastereomers were inseparable) in low to moderate yields (9–75%) but with a high level of enantioselectivity for both *syn* and *anti*-isomers (*ee*_{*syn*} 54–99% and *ee*_{*trans*} 7–98%). Interestingly, a reverse *anti*-selectivity was observed in some cases (for example for R¹ = Ph and R² = R³ = R⁴ = R⁵ = R⁶ = H or for R¹ = Me, R² = R³ = R⁴ = H, R⁵ = R⁶ = OMe). Generally speaking, a wide array of substituents was well-tolerated, except for 5-(*N*)-pyrrolidinyl substituent (no reaction), substitution of position C6 (drop of both *dr* and *ee*) and 3-methyl (low yield and *ee* but high *dr*). Then, several conditions for the reductive removal of the protecting groups from **67a** were set up to afford the corresponding tetrahydroisoquinoline **68a** or the quinoline **1a** without racemization (Scheme 19b). Finally, this dearomatization reaction was used as a key step in the multi-step synthesis of the enantioenriched 13-methyl tetrahydroprotoberberine **69a** (95% *ee*) in 18% overall yield over 8 steps from dihydroquinoline **67b** (Scheme 19c). The reaction conditions were slightly modified (100 mol% **C12**, DCM, 0 °C) to yield the corresponding dihydroisoquinoline **67c** in excellent yield (92%), high diastereoselectivity in favor of the *anti*-isomer (*anti/syn* 78:22) and excellent enantiomeric excesses for both diastereoisomers (*ee*_{*anti*} 95% and *ee*_{*syn*} 85%). Further transformations led to the enantioselective synthesis of tetrahydroprotoberberine alkaloid **69**.

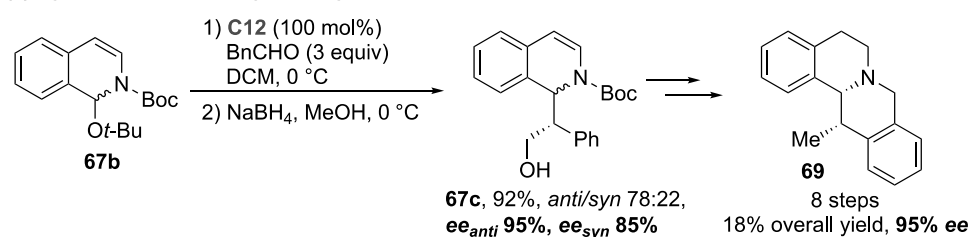
(a) Scope of the reaction



(b) Deprotection of Cbz



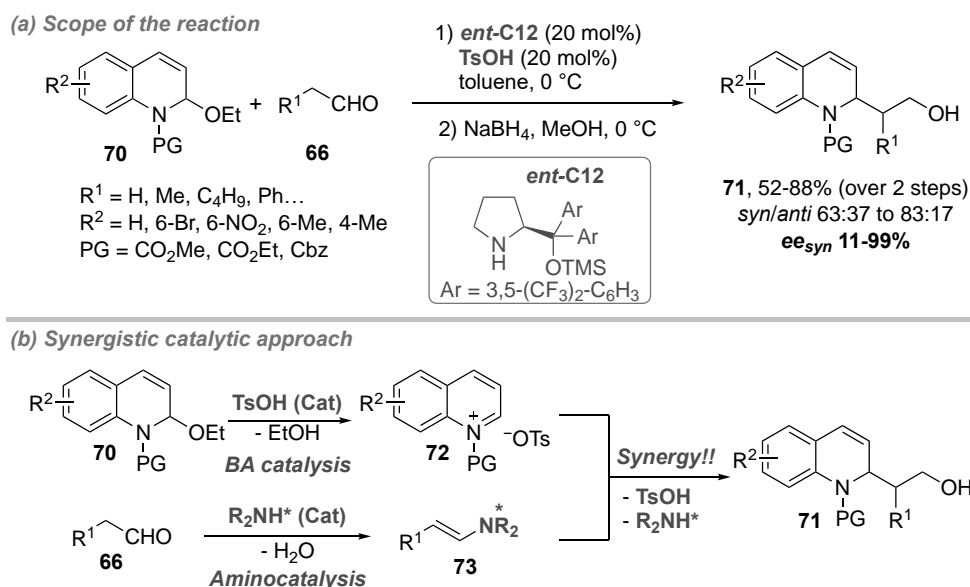
(c) Synthesis of 13-methyl tetrahydropprotoberberine alkaloid



Scheme 19. Diastereo- and enantioselective dearomatization of isoquinolines **1** catalyzed by Hayashi-Jørgensen catalyst **C12**.

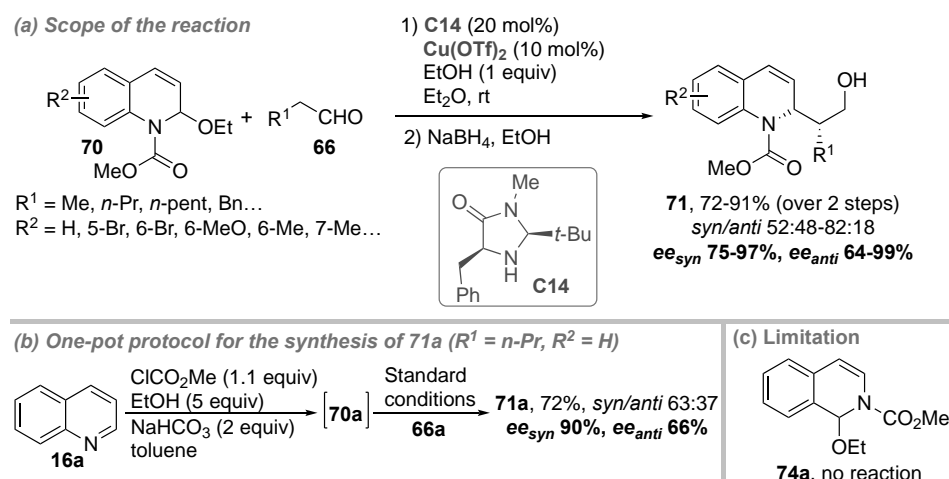
3.3. Quinolinium Salts

In 2015, the group of Pineschi tackled the enantioselective dearomatization of the quinolinium salt **72** formed in situ from N-carbamate-2-ethoxy-1,2-dihydroquinolines **70**, by nucleophilic addition of aldehydes **66** under synergistic catalytic conditions consisting of a Hayashi-Jørgensen catalyst **ent-C12** and TsOH used as a Brønsted acid (BA) (Scheme 20) [60]. By using 20 mol% of both **ent-C12** and TsOH in toluene at 0 °C followed by reduction of the carbonyl group to the corresponding alcohol, several enantioenriched dihydroquinolines **71** were obtained in moderate to high isolated yields as a mixture of syn/anti diastereomers which are, in general, inseparable (Scheme 20a). The reaction proved to be syn-selective with a moderate level of diastereoselectivity (63:37 to 83:17). Nevertheless, excellent levels of enantioselectivity (>90% ee in most cases) were observed for the syn diastereomer except when acetaldehyde (R¹ = H) was used (PG = CO₂Me or Cbz, R² = H: 11 and 25% ee respectively). Regarding the mechanism, this reaction is based upon the synergistic role of two catalysts namely (1) an aminocatalyst (**ent-C12**) able to catalytically generate a chiral enamine **73** from the corresponding aldehydes **66** and (2) a Brønsted acid (TsOH) which provides the quinolinium intermediate **72** (Scheme 20b).



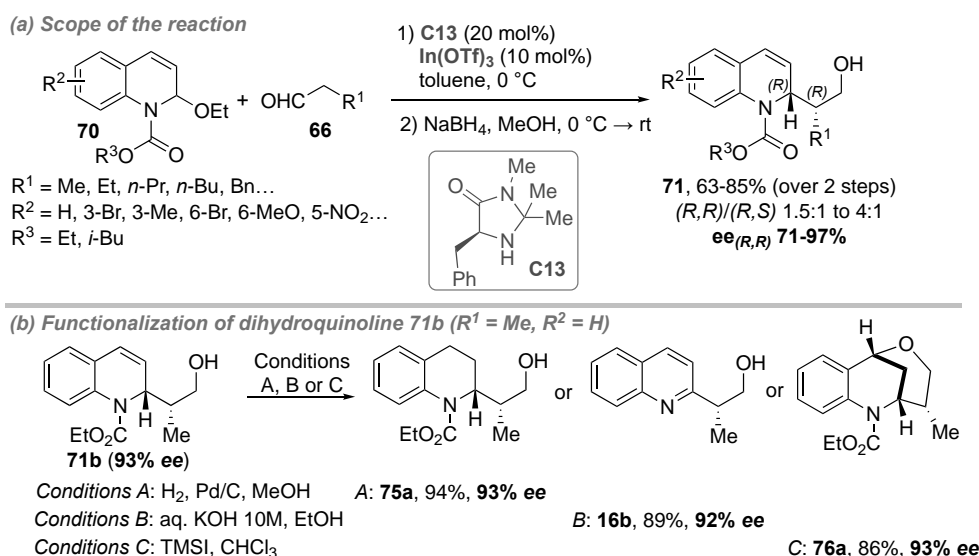
Scheme 20. Diastereo- and enantioselective dearomatization of *in situ*-formed quinolinium salt **72** via synergistic TsOH/chiral secondary amine catalyst *ent*-**C12**.

The same year and following the same synergistic strategy but in presence of a metal Lewis acid instead of a Brønsted acid, Liu et al. reported on the enantioselective dearomatization of the quinolinium salt formed *in situ* from N-carbamate-2-ethoxy-1,2-dihydroquinolines **70** by nucleophilic addition of aldehydes **66** (Scheme 21) [61]. Among all the Lewis acid/aminocatalyst couples tested, the best results were obtained by making use of $\text{Cu}(\text{OTf})_2$ (10 mol%) and imidazolidinone **C14** (20 mol%). Thus, by applying optimal conditions (1 equiv of EtOH in Et_2O at rt), several dihydroquinoline derivatives **71** were obtained after reduction of the aldehyde moiety into the corresponding alcohol (Scheme 21a). Generally speaking, high isolated yields (72–91%), modest to high drs in favor of the syn-diastereomer (52:48 to 82:18) and excellent levels of enantioselectivity (ee_{syn} 75–99%; ee_{anti} 64–99%) were obtained for a wide array of substituents on both aldehyde and quinoline partners. It is worthy of note that a one-pot protocol was set up for the synthesis of dihydroquinoline **71a** ($R^1 = n\text{-Pr}$, $R^2 = \text{H}$) from quinoline **16a** allowing the *in situ* generation of the dihydroquinoline **70a** which was then subjected to alkylation reaction under standard conditions developed above (Scheme 21b). Nevertheless, this one-pot protocol gave lower diastereo- and enantioselectivity than the classical protocol with pentanal **66b** (syn/anti 63:37, ee_{syn} 90%, ee_{anti} 66% vs syn/anti 74:26, ee_{syn} 99%, ee_{anti} 99% respectively). The absolute and relative configurations of compounds **71** were determined by X-ray single crystal analysis after esterification of the alcohol. Finally, the optimized conditions proved to be very specific to quinoline derivatives as an attempt to extend the protocol to dihydroisoquinoline **74a** failed (only traces of the desired product were observed) (Scheme 21c).



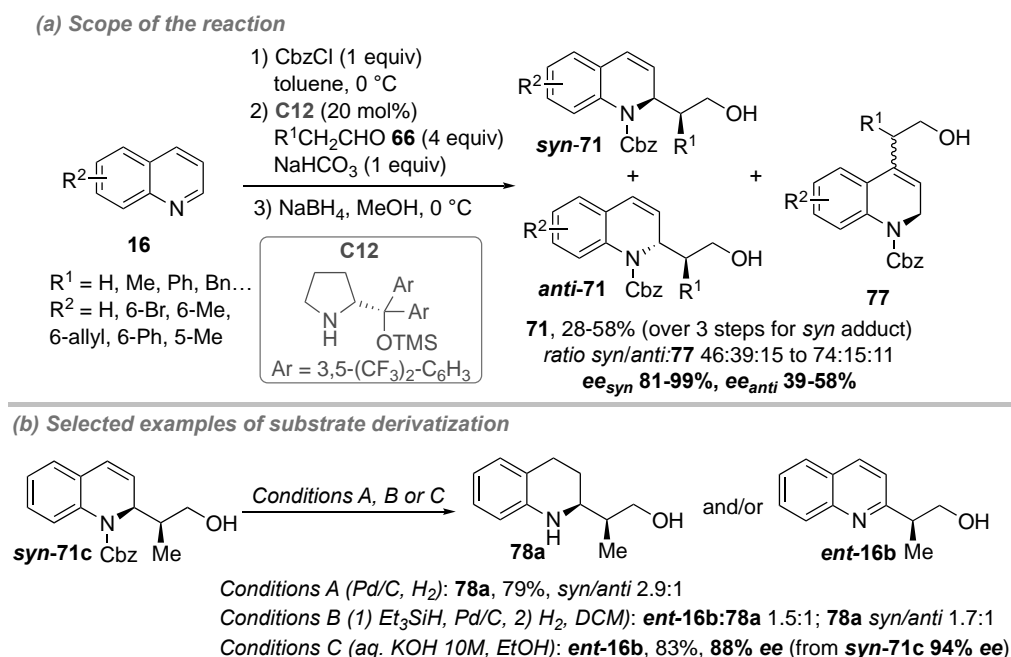
Scheme 21. Diastereo- and enantioselective dearomatization of in situ formed quinolinium salts **70** via synergistic $\text{Cu}(\text{OTf})_2$ /chiral secondary amine catalyst **C14**.

Almost simultaneously, Rueping et al. reported a rather similar approach as above by using a slightly different synergistic Lewis acid/aminocatalyst catalytic system (Scheme 22) [62]. Thus, in the presence of chiral imidazolidinone **C13** (20 mol%) and $\text{In}(\text{OTf})_3$ (10 mol%), aldehydes **66** reacted smoothly with N-carbamate-2-ethoxy-1,2-dihydroquinolines **70** providing 1,2-dihydroquinolines **71** after reduction of the aldehyde group to the corresponding alcohol with sodium borohydride. High isolated yields (63–85%) and a modest level of diastereoselectivity ($(R,R)/(R,S)$: 1.5:1 to 4:1) were obtained along with high to excellent enantioselectivity for the major (R,R) -diastereomer (71–97% *ee*) (Scheme 22a). The absolute configuration of 1,2-dihydroquinolines **71** was ascertained by X-ray single crystal analysis. Then, further derivatizations of product **71b** ($R^1 = \text{Me}, R^2 = \text{H}$) were addressed (Scheme 22b). Under hydrogenation conditions (Conditions A), tetrahydroquinoline **75a** was obtained in 94% isolated yield without racemization (93% *ee*). Under basic treatment (conditions B), a deprotection of the carbamate and a re-aromatization occurred to provide the enantioenriched quinoline **16b** in 89% isolated yield and almost no racemization (92% *ee*). Finally, under hydroetherification conditions (Conditions C), bridged quinoline **76a** was obtained in good yield and enantioselectivity (86%, 93% *ee*).



Scheme 22. Diastereo- and enantioselective dearomatization of in situ formed quinolinium salts **70** via synergistic $\text{In}(\text{OTf})_3$ /chiral secondary amine catalyst **C13**.

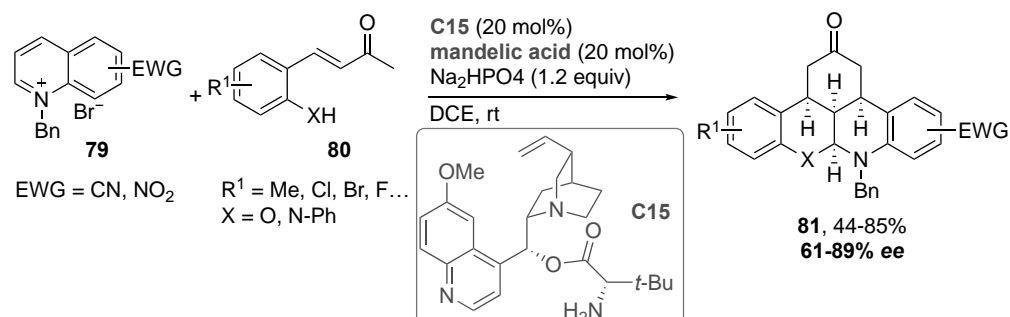
In 2016, the group of Cozzi and Gualandi reported on an organocatalytic stereoselective addition of aldehydes **66** to acylquinolinium ions catalyzed by the Hayashi–Jørgensen catalyst **C12** (Scheme 6) [63]. The one-pot sequence is divided in three steps (1) the in situ generation of the quinolinium salt by reaction between quinolines **16** and CbzCl (TrocCl failed to promote the reaction), (2) enantioselective nucleophilic addition of aldehydes **66** catalyzed by Hayashi–Jørgensen catalyst **C12**, and (3) the reduction of the aldehyde by NaBH₄. This simple procedure was then applied to several quinolines **16** and aldehydes **66** providing the corresponding 1,2-dihydroquinoline derivatives as a syn/anti mixture of separable diastereomers along with a small amount of the 1,4-dihydroquinolines derivatives **77** (**syn-71/anti-71/77** ratio: 46:39:15 to 74:15:11) (Scheme 23a). Generally speaking, low to moderate yields for the syn-adduct **syn-71** (but in agreement with the diastereoselectivity) were obtained (28–58%). Regarding the enantioselectivity, enantiomeric excesses for the syn and anti-diastereomers were excellent in all cases (77–99% *ee*, except for R¹ = Ph, *ee*_{trans} 34%). In order to demonstrate the usefulness of the 1,2-dihydroquinolines **71**, the authors have studied different derivatization conditions (Scheme 23b). Indeed, when **syn-71c** (R¹ = Me, R² = H) was submitted to hydrogenation conditions (conditions A: H₂, Pd/C), N-H tertahydroquinoline **78a** was observed in good isolated yield (79%) but as a mixture of anti/syn isomers resulting from a partial epimerization occurring during the Cbz cleavage. Others hydrogenation conditions (Conditions B: 1) Et₃SiH, Pd/C, 2) H₂, DCM) gave a 1.5:1 mixture of re-aromatized quinoline **ent-16b** and desired deprotected product **78a** (syn/anti 1.7:1). Finally, treatment of **syn-71c** (*ee*_{syn} 94%) by aqueous KOH in EtOH (conditions C) afforded the re-aromatized quinoline **ent-16b** in good yield and enantioselectivity (83%, 88% *ee*).



Scheme 23. Diastereo- and enantioselective dearomatization of quinoline **16** catalyzed by **C12**.

Recently, Chen and Du published the synthesis of polycyclic compounds **81** through a cascade reaction involving N-benzyl quinolinium salts **79** bearing an electron-withdrawing group and o-hydroxyenone derivatives **80** catalyzed by chiral primary amine organocatalyst derived for Cinchona alkaloids **C15** (Scheme 24) [64]. The reaction in the presence of 20 mol% of **C15** and 20 mol% of racemic mandelic acid co-catalyst afforded the enantioenriched polycyclic product **81** as a single diastereoisomer in modest to high isolated yields (44–85%) and high level of enantiocontrol (61–89% *ee*). Moving from an o-hydroxyenone derivatives **80** (X = OH) to an o-aminoenone derivatives **80** (X = N-Ph) was possible but

at the expense of both isolated yield and *ee* (63%, 61% *ee* vs 70%, 89% *ee* respectively). Interestingly, the presence of an electron-withdrawing group (NO₂ or CN) at position 6 or 7 was crucial from the reactivity point of view.

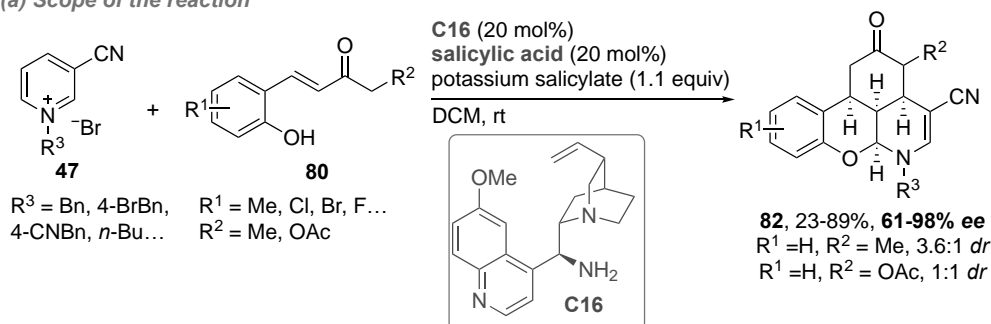


Scheme 24. Asymmetric dearomative cascade multiple functionalization of quinolinium salts **79** catalyzed by **C15**.

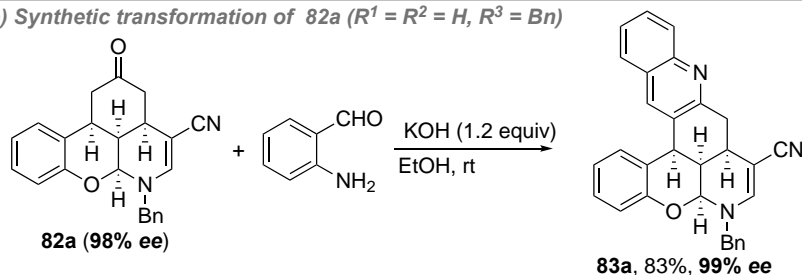
3.4. Pyridinium Salts

The approach reported by Chen and Du (see Scheme 24) proved to be quite general as pyridinium salts **47** were also tolerated after a slight modification of the reaction conditions (**C16** (20 mol%), salicylic acid (20 mol%), potassium salicylate (1.1 equiv), DCM) (Scheme 25) [64]. Polycyclic compounds **82** were thus obtained in low to high yields (23–89%) and excellent enantiomeric excesses (61–98% *ee*) (Scheme 25a). It has to be noted that for R² ≠ H, no or modest diastereoselectivity was observed (R¹ = H, R² = OAc, 3.6:1; R¹ = H, R² = OAc, 1:1). Finally, a chemical transformation of compound **82a** (R¹ = R² = H, R³ = Bn, 98% *ee*) to the more complex structure **83a** through a Friedlander reaction was performed in high isolated yield and without racemization (83%, 99% *ee*) (Scheme 25b).

(a) Scope of the reaction



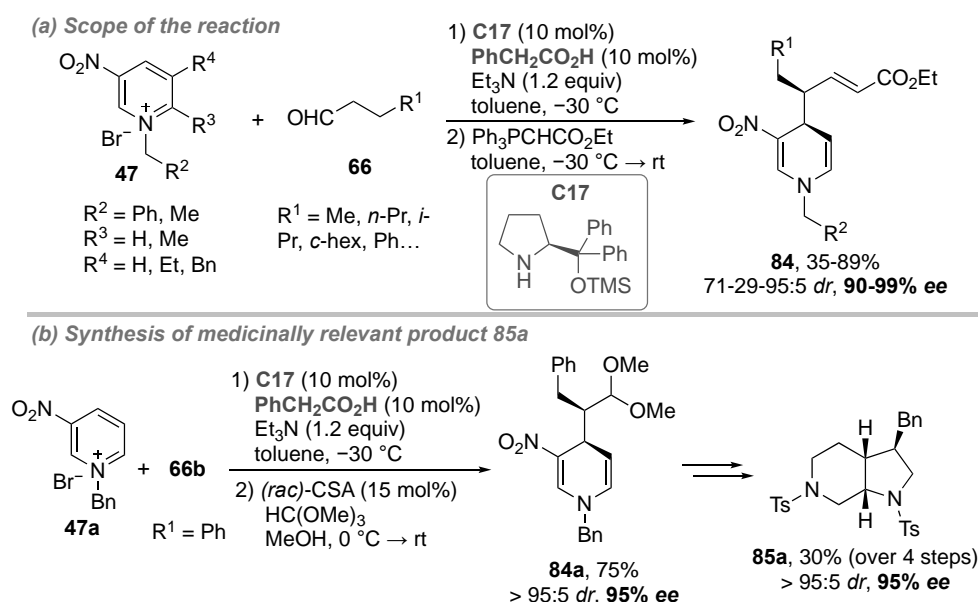
(b) Synthetic transformation of **82a** (R¹ = R² = H, R³ = Bn)



Scheme 25. Asymmetric dearomative cascade multiple functionalization of pyridinium salts **47** catalyzed by **C16**.

In 2017, Bernardi and Fochi have achieved nucleophilic dearomatization of pyridinium salts **47** under enamine catalysis using Jørgensen catalyst **C17** (10 mol%) and phenyl acetic acid (10 mol%) as co-catalyst (Scheme 26) [65]. This acid co-catalyst was proposed to buffer the unreacted amount of Et₃N at the end of the reaction thus slowing post-addition

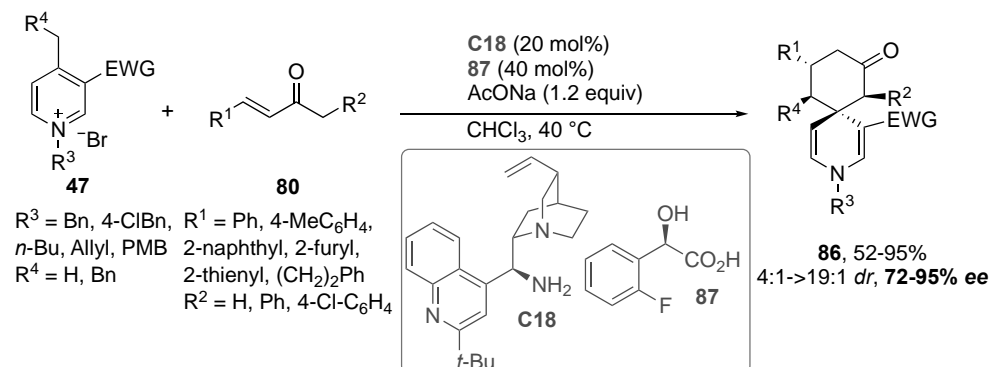
epimerization. In the presence of Et₃N (1 equiv, in order to trap HBr formed during the reaction) in toluene at −30 °C, regioselective addition at C4 position occurred to afford the enantioenriched 1,4-dihydropyridines **84** providing that the aldehyde group was transformed into α,β -unsaturated ester by Wittig reaction to solve stability issues. Thus, 1,4-dihydropyridines **84** were isolated in low to high yields (35–89%), high drs (71:29–95:5) and excellent levels of enantioselectivity (90–99% *ee*) (Scheme 26a). In most cases, the diastereomeric purity could be improved to >95:5 after purification. The relative and absolute configurations were determined by NMR and ECD spectroscopy and confirmed by X-ray diffraction analysis. In order to demonstrate the potency of their approach, the authors have tackled the synthesis of compound **85a** possessing a pyrrolo[2,3-*c*]pyridine core which is encountered in anticancer peptidomimetics (Scheme 26b). Compound **85a** was thus obtained in 30% overall yield over four steps in 95% *ee* from 1,4-dihydropyridine **84a** (75%, >95:5 dr, 95% *ee*) which was synthesized under standard conditions and transformed into the corresponding acetal in 75% yield.



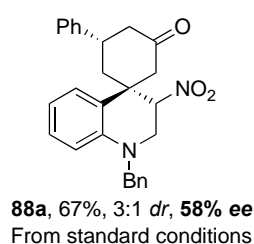
Scheme 26. Asymmetric nucleophilic dearomatization of pyridinium salts **47** catalyzed by **C17**.

In 2018, Chen and Liang have published an asymmetric dearomative formal [4 + 2] cycloaddition of enones **80** and dialkyl pyridinium salts **47** providing azaspiro[5.5]undecane scaffolds **86** thanks to an iminium ion/enamine activation sequence (Scheme 27) [66]. Thus, in the presence of chiral primary amine catalyst **C18** (10 mol%), chiral carboxylic acid **87** (40 mol%) and AcONa (1.2 equiv) in CHCl₃ at 5 °C, cycloadducts **86** were obtained in moderate to excellent yields (52–95%), diastereoselectivity (4:1–>19:1) and enantioselectivity (72–95% *ee*) (Scheme 27a). Interestingly, one example in quinolinium series was reported although the yield, *dr* and enantiomeric excess (67%, 3:1 *dr*, 58% *ee*) of product **88a** were lower than those obtained in the pyridinium series (Scheme 27b). Finally, synthetic transformations were reported starting from compound **86a** (R¹ = Ph, R² = R⁴ = H, R³ = Bn) (Scheme 27c). Under hydrogenation conditions (H₂ (2 MPa), Pd/C) in the presence of Boc₂O, reduction of the nitro group occurred concomitantly with N-debenzylation to furnish N,N'-Bis(Boc)-protected product **89a** in 80% isolated yield but with fair diastereoselectivity (2:1 *dr*) and almost no modification of the *ee* (92% *ee* and 91% *ee* respectively for the two diastereomers). Interestingly, treatment of **86a** with BF₃·Et₂O yielded the 4-methylene 1,4-dihydropyridine derivative **90a** in excellent yield and enantiomeric excess (93%, 92% *ee*).

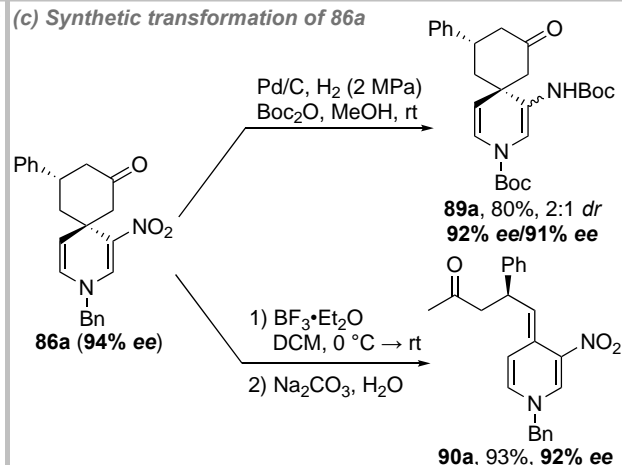
(a) Scope of the reaction



(b) Only example in quinoline series



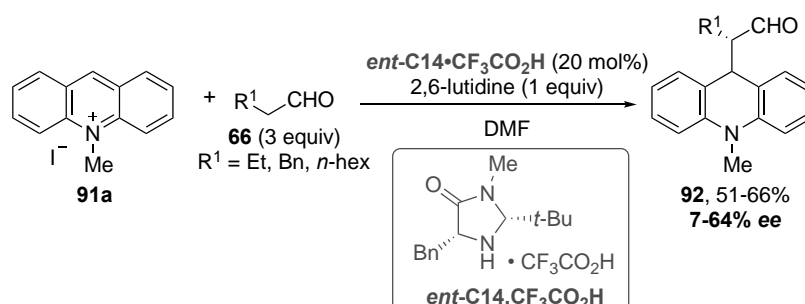
(c) Synthetic transformation of 86a



Scheme 27. Asymmetric dearomative formal [4 + 2] cycloaddition of 4-alkyl-substituted N-alkyl pyridinium salts **47** to enones **80**.

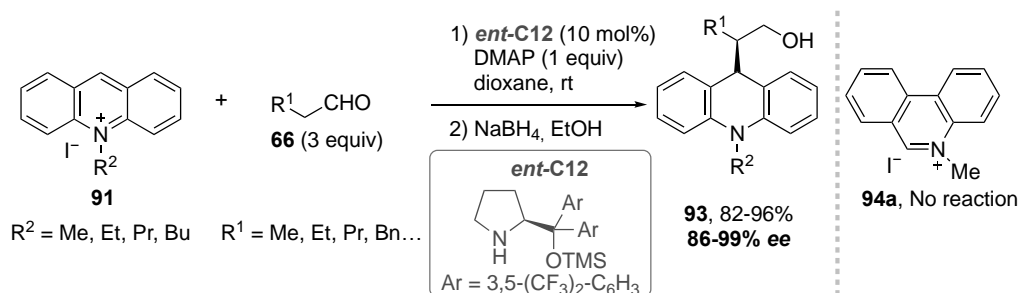
3.5. Acridinium Salts

Intermolecular 1,4-addition of aldehydes **66** to *N*-Methyl acridinium salt **91a** is seldom reported in the literature. The first example was illustrated by Cozzi et al. in 2010. Using 20 mol% of MacMillan catalyst *ent*-**C14**·**CF₃CO₂H**, the authors were able to add a few aldehydes **66** to acridinium **91** providing 1,4-dihydroacridine **92** in fair isolated yields (51–66%) and low to modest enantiomeric excesses (7–64% *ee*) (Scheme 28) [67]. The reaction conditions were found to be sensitive in terms of solvent and counter-ion as only DMF and iodide respectively allowed the reaction to occur. It is worth mentioning that reaction with hydrocinnamaldehyde ($\text{R}^1 = \text{Bn}$) led to a poor *ee* of 7%, much lower compared to octanal (64% *ee*). In order to explain this difference of behavior, the authors proposed that this gap in *ee* was due to detrimental π interactions between the aldehyde **66** and the acridinium salt **91**.



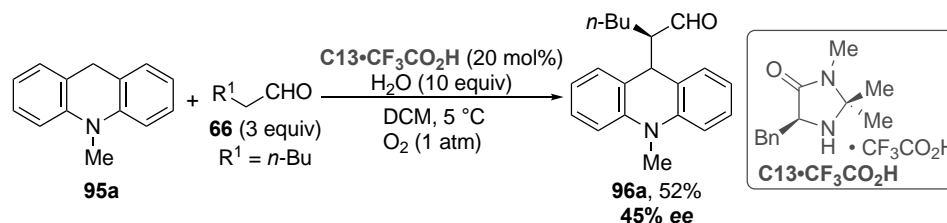
Scheme 28. Asymmetric dearomatization of acridinium salt **91a** catalyzed by *ent*-**C14**·**CF₃CO₂H**.

The group of Xiao and Li improved Cozzi's results by moving to the Jørgensen-Hayashi catalyst **ent-C12** (Scheme 29) [68]. Thus, in the presence of 10 mol% of **ent-C12** and 1 equiv of DMAP, 1,4-dihydroacridines **93** were obtained from acridinium salts **91** and aldehydes **66** in high yields (82–96%) and excellent levels of enantioselectivity (86–99% *ee*) after reduction of the aldehyde to the corresponding alcohol (NaBH₄, EtOH). It is worthy of note that *N*-methyl phenanthridinium iodide **94a** failed to provide the addition product.



Scheme 29. Asymmetric dearomatization of acridinium salt **91** catalyzed by **ent-C12**.

Instead of starting directly from acridinium salt **91a**, Zhang et al. generated the acridinium in situ by oxidation of 1,4-dihydroacridine **95a** under O₂ atmosphere [69]. In this case, using 20 mol% of MacMillan's catalyst **C13**·CF₃CO₂H, a moderate isolated yield (52%) and enantiomeric excess (45% *ee*) could be obtained for the substituted 1,4-dihydroacridine **96a** despite good results were achieved with xanthene (O instead of *N*-Me) (Scheme 30).



Scheme 30. Asymmetric dearomatization of acridinium salt formed in situ from **95** catalyzed by **C13**·CF₃CO₂H.

4. Nucleophilic Catalysis

The asymmetric dearomatization process based on nucleophilic catalysis has met important developments while addressing major selectivity issues. First of all, these organocatalytic strategies led to the dearomatization of two kinds of heterocyclic architectures such as *N*-iminoazolum ylide derivatives (Figure 4, case **A**) and pyridinium salt derivatives (Figure 4, case **B**) which underwent either C2 or C4-addition reaction as formal electrophilic species. Most of the work has been achieved by means of NHC catalysis which highlighted enolate or homoenolate type of chemistry of Breslow intermediates (Figure 4, cases **C** and **D**) together with acylation reactions (Figure 4, case **E**). On the other hand, the phosphine-based catalysis, encompassing the addition to allenes in order to generate phosphonium zwitterionic species, has met fewer but important achievements for the dearomatization of *N*-iminoazolum ylide compounds (Figure 4, case **F**). Finally, isothioureia catalysis allows the nucleophilic addition of C(1)-ammonium enolate intermediates generated by the addition of the catalyst to substituted phenyl acetate derivatives (Figure 4, case **G**).

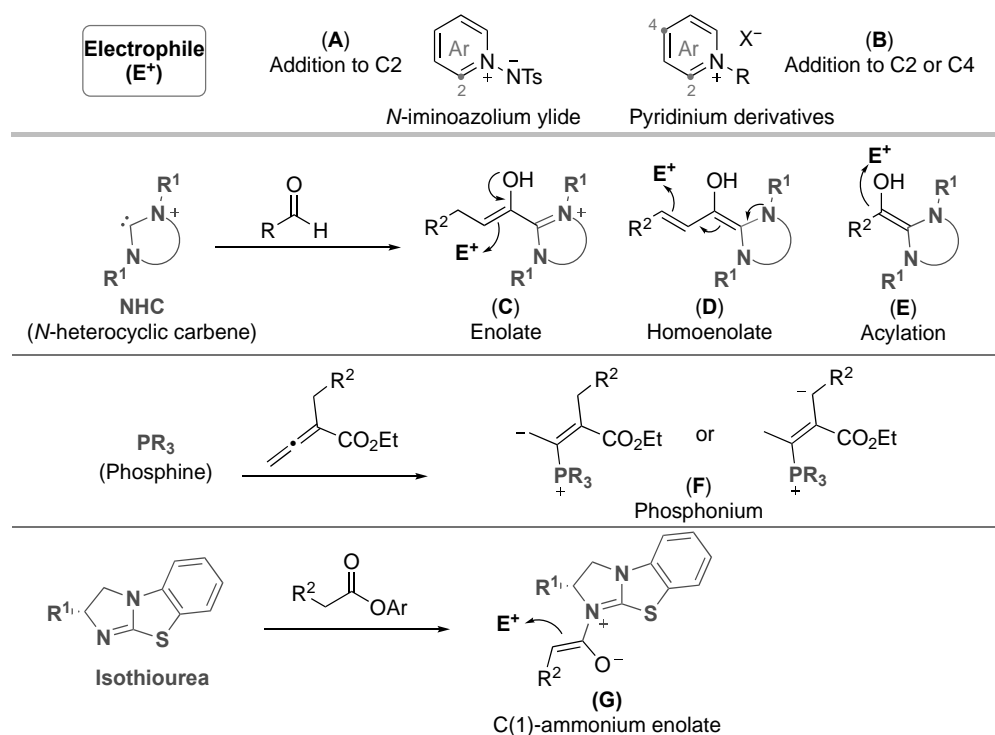
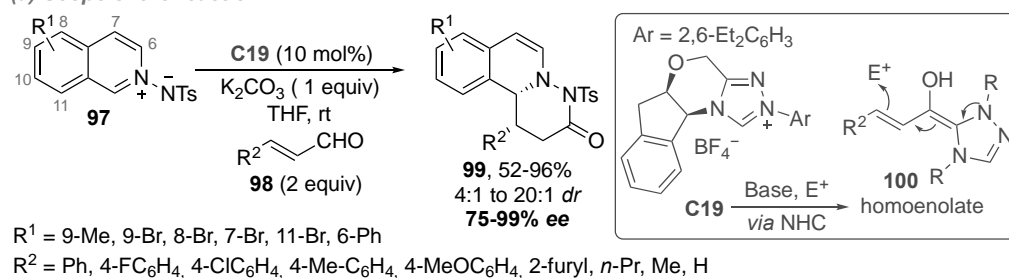


Figure 4. Dearomatization by nucleophilic catalysis: an Overview.

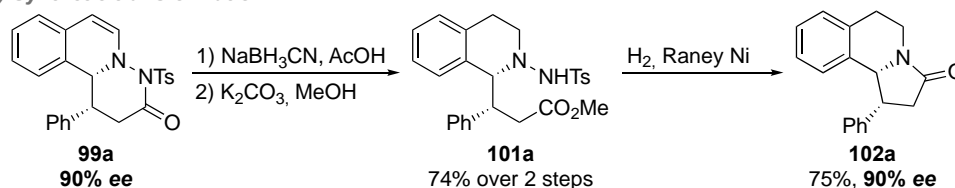
4.1. Isoquinolinium Salts

The group of Glorius tackled the dearomatization sequence of *N*-iminoisoquinolinium ylides **97** by means of unsaturated aldehydes **98** and the triazolinium salt **C19** as a *N*-heterocyclic carbene (NHC) precursor (Scheme 31) [70]. In the presence of K_2CO_3 as a base, the NHC catalyst was generated to form the transient homoenolate species **4** upon the addition sequence onto aldehydes **98**, leading subsequently to a (3 + 3) cycloaddition with azomethine imines **97** allowing the formation of lactams **99** with high *ees* and good diastereoselectivities (Scheme 31a). The authors showed that lactam **99a** underwent a facile reductive-ring opening sequence to give the corresponding ester **101a** (Scheme 31b). Under reductive conditions (H_2 , Raney Ni), allowing the nitrogen-nitrogen bond cleavage, the pyrrolidinone derivative **102a** was eventually synthesized, without loss of *ee*, and displays the polycyclic structure of indolizidine alkaloids proving thereby the utility of these compounds. Worthy of note, this enantioselective process was also demonstrated during the dearomatization of *N*-iminopyridinium yield which complements the developments described below in Section 4.2.

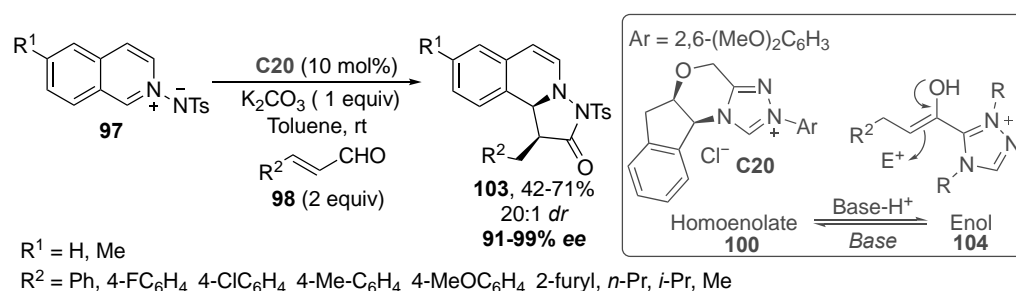
(a) Scope of the reaction



(b) Synthetic transformation

Scheme 31. (3 + 3) cycloaddition to azomethine imines **97** catalyzed by NHC.

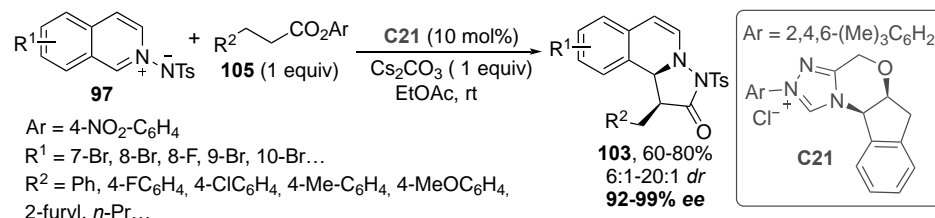
The authors investigated in detail the reaction conditions highlighting that the basicity of the base in a given solvent markedly influences the reaction pathway [70]. Indeed, moving from THF to toluene and in the presence of the pre-catalyst **C20**, it was observed that the homoenolate intermediate **100** was in equilibrium with the enolate **104** (Scheme 32), the latter leading to a (3 + 2) cycloaddition onto the *N*-iminoisoquinolinium **97**. Thus, the pyrrolidinones **103** were obtained in excellent *ees* and *dr* in a diversity-oriented synthesis fashion from the same precursors **97** and **98** (Scheme 32 vs. Scheme 31). Wang, Wei et al. performed DFT calculations on these novel sequences and proved that K_2CO_3 was a suited base to secure the equilibrium between homoenolate-enol species (**100** vs. **104**) while the stereoselectivity issues would stem from π - π and hydrogen bonding interactions with NHC intermediates [71].

Scheme 32. (3 + 2) cycloaddition to azomethine imines **97** catalyzed by NHC.

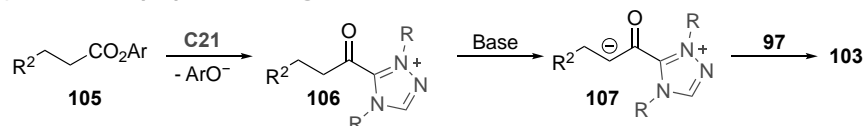
In 2018, Liu and Xu reported on a (3 + 2) dearomatizing annulation of *N*-iminoisoquinolinium ylides **97** by saturated carboxylic esters **105** in the presence of the triazolium salt **C21** as a *N*-heterocyclic carbene (NHC) precursor following a similar approach as reported by Glorius (Scheme 33) [72]. The pyrrolidinones **103** were thus obtained in good isolated yield and *dr* (60–80%, 6:1–20:1) and excellent levels of enantioselectivity (92–99% *ee*) for a wide array of substituents on both ester and *N*-iminoisoquinolinium ylide partners (Scheme 33a). Indeed, in this case, the enolate intermediate **107** was generated after the addition of the NHC catalyst to the phenolic ester **105** followed by a deprotonation with Cs_2CO_3 . The reactive enolate led to nucleophilic addition to the electrophilic carbon of the *N*-iminoisoquinolinium ylide **97** (Scheme 33b). Synthesis of indolizidine derivatives **108**, important structural motifs in natural alkaloids, was then tackled by implementing a simple reduction of the double bond of **103** in moderate isolated yields (60 and 62%), high

dr (10:1 and 8:1) and with almost no racemization (95% and 97% *ee* from 99% and 96% *ee* respectively) (Scheme 33c).

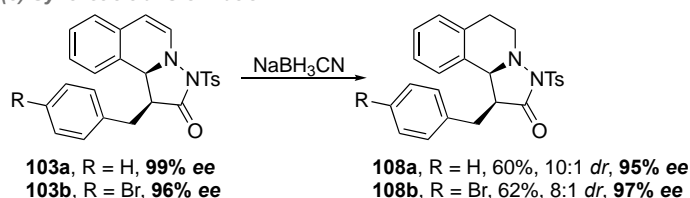
(a) Scope of the reaction



(b) Mechanistic proposal for the generation of reactive enolate intermediate

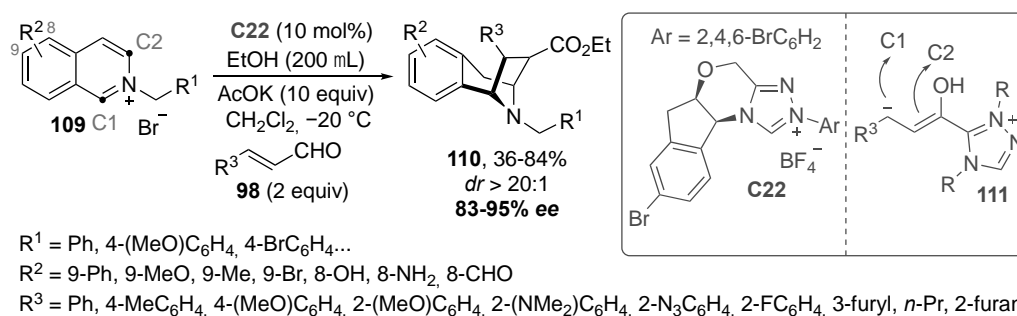


(c) Synthetic transformation



Scheme 33. (3 + 2) cycloaddition of unsaturated carboxylic esters **105** to azomethine imines **97** catalyzed by NHC.

Tan et al. envisaged an alternative dearomatization sequence making use of the two electrophilic sites at C1 and C2 of isoquinolinium salts **109** (Scheme 34) [73]. Then, upon NHC catalysis, from the triazolium precursor **C22** and unsaturated aldehydes **98**, the formal reactive species **111** was formed and able to trigger a double Mannich-type reaction to isoquinolinium salt **109**. Thus, the tropane derivatives **110**, displaying a known bridge-skeleton of naturally occurring and bioactive compounds, were obtained in a complete diastereoselectivity and excellent *ees*. Although a large array of compounds was constructed, this reaction proceeded essentially from α,β -unsaturated aldehydes **98** flanked by an aromatic moiety. The one-pot, albeit stepwise four components sequence, was also successfully developed by the *in-situ* formed isoquinolinium precursor **109** followed by the addition of the other components. Based on the recent DFT computational investigations by Qu, Wei and colleagues, this domino reaction is believed to proceed through a stepwise fashion starting with the regio- and enantioselective Mannich reaction at C1, followed by the diastereoselective cyclization [74]. Importantly, the use of ethanol as an additive was crucial to secure the ethanolysis event of the acyltriazolium intermediate **C22** in order to regenerate the NHC catalyst.

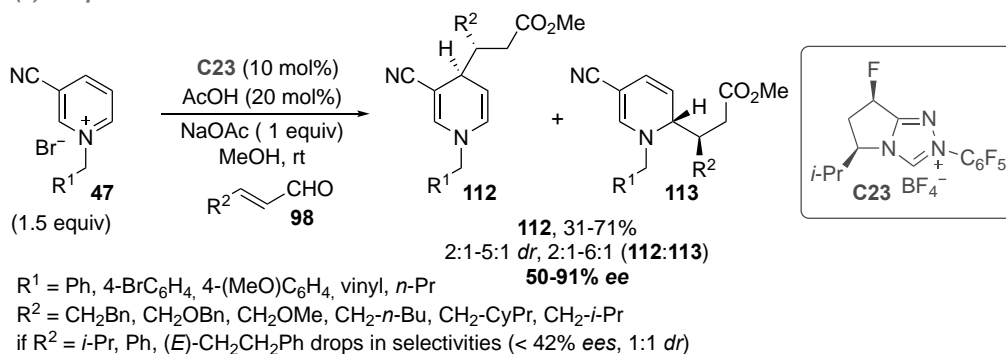


Scheme 34. Double Mannich reaction to isoquinolinium salts **109** catalyzed by NHC.

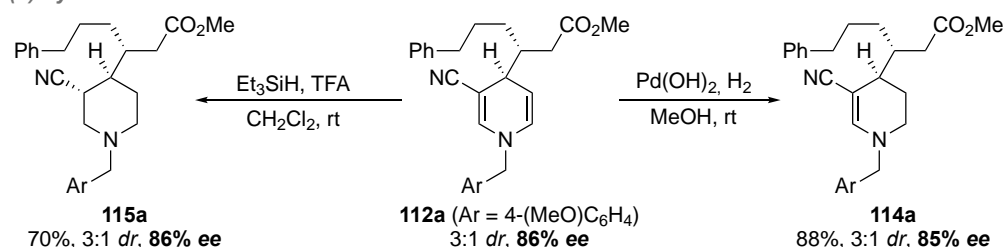
4.2. Pyridinium Salts

The dearomatization of pyridinium salts allows a versatile entry to biologically relevant dihydropyridines, while having to overcome regioselective issues in connection to the differentiation of the C2 and C4 electrophilic positions. The group of Rovis tackled the C4-selective addition reaction of Breslow intermediates, such as homoenolates **100** (see Scheme 31), generated from unsaturated aldehydes **98** upon the catalytic reaction of triazolium **C23** as an NHC precursor (Scheme 35) [75]. Several key parameters were adjusted to succeed in this process such as (1) the exploitation of activated pyridinium salt **47** having a cyano group at C3 (an acetyl led to lower selectivities), (2) the strict exclusion of oxygen and the use of acetic acid additive (*vide infra*). Then, the major 1,4-dihydropyridine products **112** were obtained in moderate to good yields (31–71%) and good *ees* (up to 91%), in parallel to the minor regioisomer **113** (Scheme 35a). The best results were observed with non-hindered aldehydes **98**, whereas counterparts **98** with $R^2 = i\text{-Pr}$ and Ar led to decreased selectivities. A mechanistic insight, thanks to labeling experiments, led the authors to propose a competitive addition of the transient carbene (formed from **C23**) to the pyridinium salt, giving aza-Breslow intermediates which could equilibrate back to starting material thanks to the use of acetic acid. Subsequently, DFT computation allowed to address the selectivity issues by showing that the largest electrophilic value was found at the C4-position of the pyridinium salt **47a** ($R = \text{Ph}$), while the enantioselective addition was controlled by hydrogen bonding like $\text{C-H}\cdots\text{F}$ and $\text{O-H}\cdots\text{N}$ [76]. In order to showcase the obtained dihydropyridines such as **112a**, the authors demonstrated the possibility to reduce selectively either partially (with $\text{Pd}(\text{OH})_2$, H_2 giving **114a**) or completely (Et_3SiH , TFA giving **115a**) one or the two C–C double bonds to provide tetrahydropyridine **114a** or piperidine **115a** respectively without altering the enantiomeric excess of the starting material **112a** (Scheme 35b).

(a) Scope of the reaction



(b) Synthetic transformations

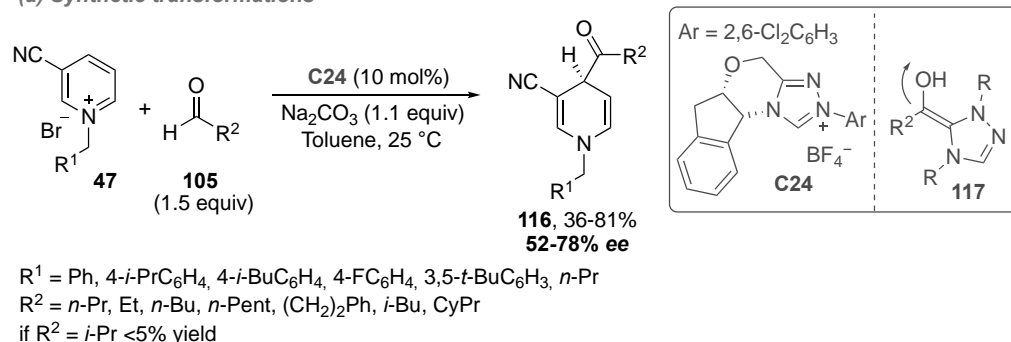


Scheme 35. C4-selective addition of **98** to pyridinium salts **47** catalyzed by NHC.

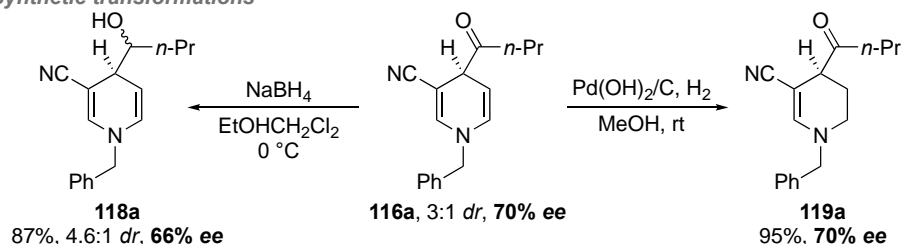
In the same vein, the group of Mazzanti has reported on an efficient dearomatization sequence of *N*-benzyl pyridinium **47** upon the formal addition reaction of aldehydes **105**, provided that a cyano functional group was present at the C3 position; other EWG did not afford any reaction (Scheme 36) [77]. A screening of various pre-NHC catalysts revealed that triazolium **C24** was competent to generate the so-called Breslow intermediate **117** in the presence of Na_2CO_3 as a base leading, eventually, to 1,4-dihydropyridines **116** with a

complete regioselectivity and *ees* up to 78% (Scheme 36a). The best selectivities (>70% *ee*) were obtained with aliphatic aldehydes bulkier than $R^2 = \text{Et}$ (60% *ee* for $R^1 = \text{Ph}$) but the *ees* dropped with α -branched aldehydes as testified with cyclopropyl derivatives giving 52% *ee* ($R^1 = \text{Ph}$, $R^2 = \text{CyPr}$) while the one with $R^2 = i\text{-Pr}$ did not allow any conversion. Contrariwise to the aforementioned Rovis achievement [45], the authors demonstrated that their conditions did not furnish any addition reaction of cinnamaldehyde and the competitive addition of the transient carbene was ruled out. In order to showcase the use of these substrates, selective reduction of the ketone moiety with NaBH_4 (**118a**, 87% yield) was carried out while the hydrogenation of the C–C double bond occurred in the presence of Pearlman palladium-based catalyst giving rise to the tetrahydropyridine **119a** in 95% and 70% *ee* (Scheme 36b).

(a) Synthetic transformations



(b) Synthetic transformations

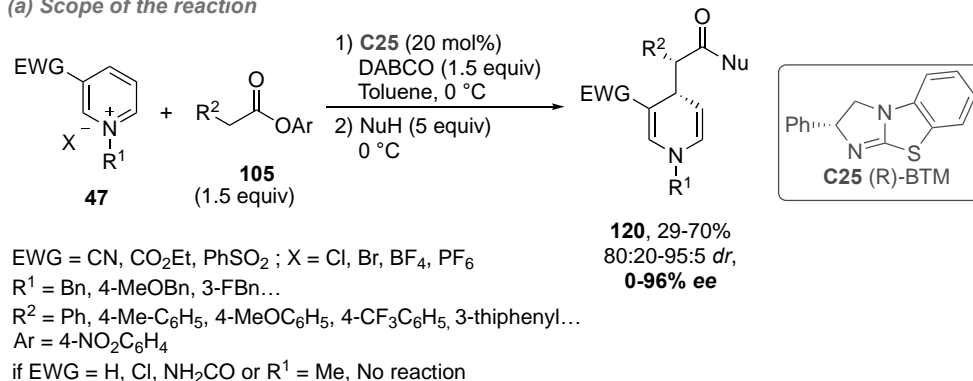


Scheme 36. Highly selective C4-acylation of pyridinium salts **47** catalyzed by NHC.

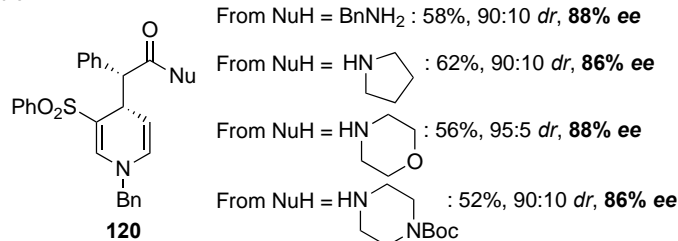
Very recently, the group of Smith has studied the synthesis of 1,4-dihydropyridines **120** by addition of aryl ester **105** to *N*-alkyl pyridinium salts **47** bearing an electron-withdrawing group at the 3-position catalyzed by (*R*)-BTM isothiourea chiral catalyst **C25** (Scheme 37) [78]. In the presence of 20 mol% of **C25**, 1.5 equivalent of DABCO in toluene at 0 °C, the reaction proceeded smoothly to provide several 1,4-addition products in low to moderate isolated yields (29–70%), good diastereoselectivities (80:20 to 95:5 *dr*) and variable level of enantioselectivity (0–96% *ee*) (Scheme 37a). For stability purposes, the 1,4-addition product **120** bearing a phenolic moiety must be transformed into the corresponding amide prior to purification by treatment of the crude mixture with amine nucleophile (benzyl amine, piperidine, morpholine or *N*-Boc piperazine) (Scheme 37b). In addition, some interesting features were noticed by the authors: 1) contrarywise to most others reported approaches which have been shown to be sensitive to variation of the EWG group of the pyridinium salt, CN, PhSO_2 and CO_2Et -substituted pyridinium salts were efficient in terms of reactivity and selectivity (except for CO_2Et which result in the production of a racemate); (2) the R^1 group must be a benzyl (pyridinium salt with Me substituent being unreactive) presumably to provide stabilization of the transition state thanks to π – π or π –cation interactions; (3) the nature of the counter-cation of the pyridinium salt is crucial for the reaction to occur. Non-coordinating anions (BF_4 or PF_6) were less efficient both in terms of enantioselectivity and reactivity than halide ones (Cl or Br). This phenomenon was tentatively attributed to the capability of the alkyl ammonium salts to act as H-bonding donors that bind to the halides ions thanks to $^+\text{NC-H}\cdots\text{X}^-$ interactions. From a mechanistic

point of view, the reaction proceeds through the formation of a C(1)-ammonium enolate intermediate resulting from the nucleophilic addition of the catalyst **C25** to the aryl ester **105** followed by deprotonation by the DABCO used as a Brønsted base (Scheme 37c).

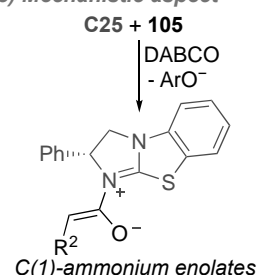
(a) Scope of the reaction



(b) Variation of NuH



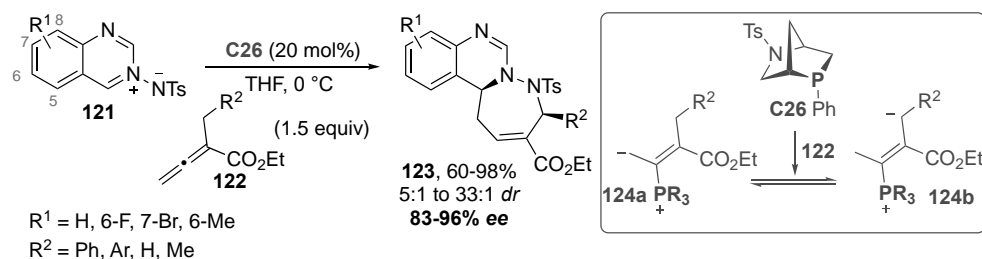
(c) Mechanistic aspect



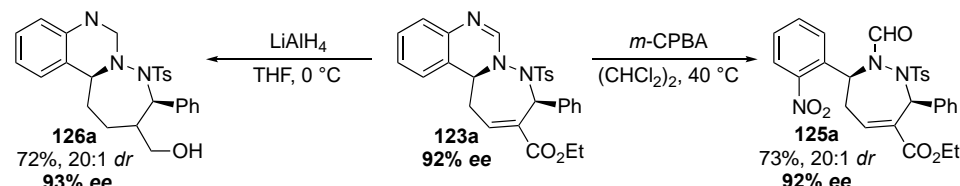
Scheme 37. C4-addition of aryl esters **105** to *N*-alkyl pyridinium salts **47** catalyzed by NHC.

4.3. Others

Quinazoline derivatives are useful building blocks in synthesis while the core structure is found in numerous bioactive compounds. In this context, Guo et al. designed an original [4+3] annulation to quinazoline derived cyclic azomethine imines **121** in order to build the corresponding seven-membered ring heterocyclic products **123** (Scheme 38) [79]. It was found that commercially available Kwon's phosphine **C26** catalyzed efficiently the addition reaction of allenates **122** to dipole **121** in a regioselective fashion, through the likely catalytic formation of phosphonium enolate zwitterion species **124** involving complex prototropic events. Then, a large range of tricyclic products **123** were obtained in excellent yields and *ees* up to 96% (Scheme 38a). The authors performed various synthetic transformations among which the oxidative cleavage of the imine motif of **123a** upon the influence of *meta*-chloroperbenzoic acid as oxidant, to give the nitro-aldehyde product **125a** for instance (Scheme 38b). Next, it was demonstrated that the reduction of the acrylate moiety of **123a** could occur in the presence of lithium aluminum hydride reagent to yield **126a** (72%, 93% *ee*). During all these transformations, the *ees* and *dr* were preserved.



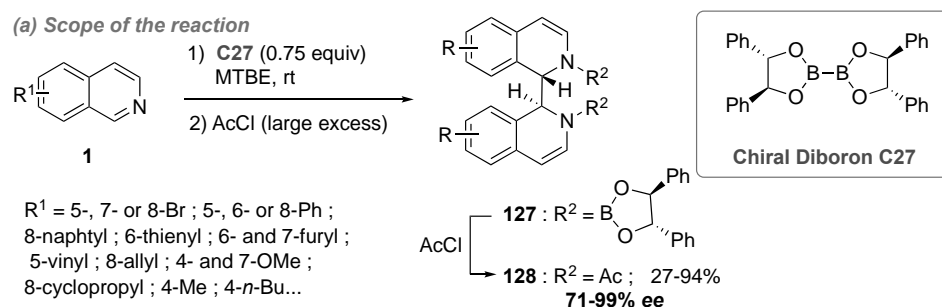
Synthetic transformations



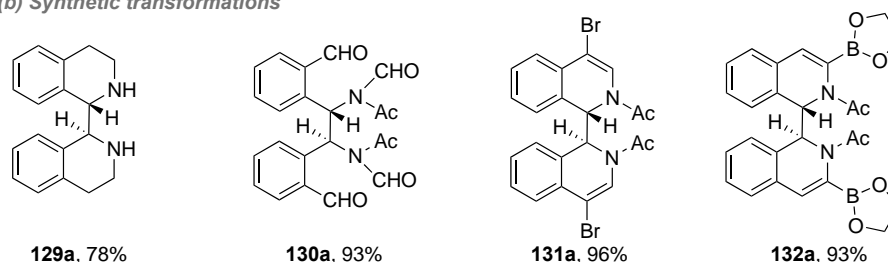
Scheme 38. (4 + 3) cycloaddition between azomethine imines derivatives **121** and allenates **122** catalyzed by NHC.

5. Miscellaneous

In 2017, an asymmetric reductive coupling of isoquinolines **1** promoted by a chiral diboron compound **C27** was reported by Tang et al., providing expeditious access to a large variety of substituted bisoquinoline **127** (20 examples) in moderate to good yields (27–94%) with complete diastereoselectivity and excellent level of enantioselectivity (71–99% ee) (Scheme 39a) [80]. The best results were obtained using the chiral diboron reagent **C27** derived from (1*S*,2*S*)-1,2-diphenylethane-1,2-diol. The labile coupling product intermediate **127** was stabilized by adding AcCl at the end of the reaction to afford the corresponding more stable bisoquinoline diacetamide **128**. A mechanistic investigation led the authors to rule out a radical mechanism and to suggest a (3,3)-sigmatropic rearrangement via a 6-membered chair-form transition state involving two isoquinolines **1** and a single diboron **C27** as the template. From bisoquinoline **128a** ($\text{R} = \text{H}$), further useful synthetic transformations could be conducted such as hydrogenation affording the cyclic diamine **129a** (78%) or the ozonolysis providing acyclic diamine **130a** (93%), as well as bromination (**131a**: 96%) and borylation (**132a**: 49%) at 4,4'- and 3,3'-position respectively (Scheme 39b).



(b) Synthetic transformations



Scheme 39. Asymmetric reductive coupling of isoquinolines **1** catalyzed by chiral diboron **C27**.

6. Conclusions

Despite the long-standing interest towards the dihydroazaarenes (pyridine, (iso)quinoline and acridine principally) which are interesting scaffolds encountered in several naturally occurring compounds, the stereoselective access to such architectures is still a challenging goal. In that context, nucleophilic dearomatization of azaarenium salts has emerged as a versatile choice. Nevertheless, several problems remain to be addressed such as (1) the regioselectivity of the addition of the nucleophilic species, (2) the lack of electrophilicity of the azaarenium salts thus requiring an extra-activation and (3) of course the control of the stereoselective outcome of the dearomatization event. To address these current limitations, organocatalytic processes were successfully designed by capitalizing on the full range of activation modes reported in the literature, including ion-binding catalysis, aminocatalysis and nucleophilic catalysis. Indeed, thanks to covalent and/or non-covalent interactions between the catalyst and the substrates, transition states with a high degree of organization allow excellent control of both regio- and stereoselectivities. It is worthy of note that the panel of nucleophiles eligible to the organocatalyzed nucleophilic dearomatization still remains limited. Thus, there is still a need for the development of enantioselective catalytic approaches. One can imagine that in the near future, new synthetic methodology merging organocatalysis and different modes of activation such as photocatalysis or organic electrosynthesis will emerge thus allowing to pave the way to a larger array of suited nucleophiles.

Author Contributions: Conceptualization, C.S. and S.O.; writing—original draft preparation, writing—review and editing, C.S., P.-A.N., J.-F.B., V.L. and S.O.; supervision, J.-F.B., V.L. and S.O.; funding acquisition, S.O. All authors have read and agreed to the published version of the manuscript.

Funding: P.-A.N. thanks the Labex SynOrg for a grant. C.S. thanks the MNERT for a grant. This work has been partially supported by the University of Rouen Normandy, INSA Rouen Normandy, the Centre National de la Recherche Scientifique (CNRS), European Regional Development Fund (ERDF), Labex SynOrg (ANR-11-LABX-0029), the graduate school for research XL-Chem (ANR-18-EURE-0020 XL CHEM), and by Region Normandie.

Conflicts of Interest: The authors declare no conflict of interest.

Abbreviations and Symbols

Cbz	benzyloxycarbonyl
CSA	camphorsulfonic acid
Boc	<i>tert</i> -butyloxycarbonyl
DCM	dichloromethane
DMAP	4-dimethylaminopyridine
MMPP	magnesium monoperoxyphthalate hexahydrate
MTBE	methyl <i>tert</i> -butyl ether
NHC	<i>N</i> -heterocyclic carbene
PIFA	[bis(trifluoroacetoxy)-iodo]benzene
TBS	<i>tert</i> -butyl(dimethyl)silyl
TFA	trifluoroacetic acid
Troc	2,2,2-trichloroethoxycarbonyl
Ts	tosyl

References

1. Roche, S.P.; Porco, J.A. Dearomatization Strategies in the Synthesis of Complex Natural Products. *Angew. Chem. Int. Ed.* **2011**, *50*, 4068–4093. [[CrossRef](#)] [[PubMed](#)]
2. Satoh, N.; Akiba, T.; Yokoshima, S.; Fukuyama, T. A practical synthesis of (–)-oseltamivir. *Angew. Chem. Int. Ed.* **2007**, *46*, 5734–5736. [[CrossRef](#)]
3. Lavilla, R. Recent developments in the chemistry of dihydropyridines. *J. Chem. Soc. Perkin Trans.* **2002**, *1*, 1141–1156. [[CrossRef](#)]
4. Auria-Luna, F.; Marqués-López, E.; Herrera, R.P. Organocatalytic Enantioselective Synthesis of 1,4-Dihydropyridines. *Adv. Synth. Catal.* **2017**, *359*, 2161–2175. [[CrossRef](#)]

5. Thu Pham, H.; Chataigner, I.; Renaud, J.-L. New Approaches to Nitrogen Containing Heterocycles: Enantioselective Organocatalyzed Synthesis of Dihydropyridines (DHP's), Quinolizidine Derivatives and Dihydropyrimidines (DHPM's). *Curr. Org. Chem.* **2012**, *16*, 1754–1775. [[CrossRef](#)]
6. Rucins, M.; Plotniece, A.; Bernotiene, E.; Tsai, W.-B.; Sobolev, A. Recent Approaches to Chiral 1,4-Dihydropyridines and their Fused Analogues. *Catalysts* **2020**, *10*, 1019. [[CrossRef](#)]
7. Faisca Phillips, A.M.; Pombeiro, A.J. Recent advances in organocatalytic enantioselective transfer hydrogenation. *Org. Biomol. Chem.* **2017**, *15*, 2307–2340. [[CrossRef](#)]
8. Kim, A.N.; Stoltz, B.M. Recent Advances in Homogeneous Catalysts for the Asymmetric Hydrogenation of Heteroarenes. *ACS Catal.* **2020**, *10*, 13834–13851. [[CrossRef](#)] [[PubMed](#)]
9. Xia, Z.L.; Xu-Xu, Q.F.; Zheng, C.; You, S.L. Chiral phosphoric acid-catalyzed asymmetric dearomatization reactions. *Chem. Soc. Rev.* **2020**, *49*, 286–300. [[CrossRef](#)] [[PubMed](#)]
10. Poddubnyi, I.S. Regioselectivity of the reactions of pyridinium and quinolinium salts with various nucleophiles (Review). *Chem. Heterocycl. Comp.* **1995**, *31*, 682–714. [[CrossRef](#)]
11. Ahamed, M.; Todd, M.H. Catalytic Asymmetric Additions of Carbon-Centered Nucleophiles to Nitrogen-Containing Aromatic Heterocycles. *Eur. J. Org. Chem.* **2010**, *2010*, 5935–5942. [[CrossRef](#)]
12. Bull, J.A.; Mousseau, J.J.; Pelletier, G.; Charette, A.B. Synthesis of pyridine and dihydropyridine derivatives by regio- and stereoselective addition to N-activated pyridines. *Chem. Rev.* **2012**, *112*, 2642–2713. [[CrossRef](#)] [[PubMed](#)]
13. Zhuo, C.X.; Zhang, W.; You, S.L. Catalytic asymmetric dearomatization reactions. *Angew. Chem. Int. Ed.* **2012**, *51*, 12662–12686. [[CrossRef](#)] [[PubMed](#)]
14. Ding, Q.; Zhou, X.; Fan, R. Recent advances in dearomatization of heteroaromatic compounds. *Org. Biomol. Chem.* **2014**, *12*, 4807–4815. [[CrossRef](#)]
15. Gualandi, A.; Mengozzi, L.; Manoni, E.; Cozzi, P.G. Stereoselective Organocatalytic Addition of Nucleophiles to Isoquinolinium and 3,4-dihydroisoquinolinium Ions: A Simple Approach for the Synthesis of Isoquinoline Alkaloids. *Catal. Lett.* **2014**, *145*, 398–419. [[CrossRef](#)]
16. Ramachandran, G.; Sathiyarayanan, K. Dearomatization Strategies of Heteroaromatic Compounds. *Curr. Organocatalysis* **2015**, *2*, 14–26. [[CrossRef](#)]
17. Liu, W.; Liu, S.; Jin, R.; Guo, H.; Zhao, J. Novel strategies for catalytic asymmetric synthesis of C1-chiral 1,2,3,4-tetrahydroisoquinolines and 3,4-dihydro-1,2,3,4-tetrahydroisoquinolines. *Org. Chem. Front.* **2015**, *2*, 288–299. [[CrossRef](#)]
18. Bertuzzi, G.; Bernardi, L.; Fochi, M. Nucleophilic Dearomatization of Activated Pyridines. *Catalysts* **2018**, *8*, 632. [[CrossRef](#)]
19. Sharma, U.K.; Ranjan, P.; Van der Eycken, E.V.; You, S.L. Sequential and direct multicomponent reaction (MCR)-based dearomatization strategies. *Chem. Soc. Rev.* **2020**, *49*, 8721–8748. [[CrossRef](#)]
20. Xia, Y.; Hu, F.; Jia, J. Transition-Metal-Catalyzed Nucleophilic Dearomatization of Electron-Deficient Heteroarenes. *Synthesis* **2021**. [[CrossRef](#)]
21. Dalko, P.I.; Moisan, L. Enantioselective Organocatalysis. *Angew. Chem. Int. Ed.* **2001**, *40*, 3726–3748. [[CrossRef](#)]
22. Dalko, P.I.; Moisan, L. In the golden age of organocatalysis. *Angew. Chem. Int. Ed.* **2004**, *43*, 5138–5175. [[CrossRef](#)]
23. Ooi, T.; Maruoka, K. Asymmetric organocatalysis of structurally well-defined chiral quaternary ammonium fluorides. *Acc. Chem. Res.* **2004**, *37*, 526–533. [[CrossRef](#)] [[PubMed](#)]
24. Berkessel, A.; Gröger, H. *Asymmetric Organocatalysis*; Wiley-VCH Verlag GmbH: Weinheim, Germany, 2005.
25. Seayad, J.; List, B. Asymmetric organocatalysis. *Org. Biomol. Chem.* **2005**, *3*, 719–724. [[CrossRef](#)] [[PubMed](#)]
26. Beeson, T.D.; Mastracchio, A.; Hong, J.B.; Ashton, K.; Macmillan, D.W. Enantioselective organocatalysis using SOMO activation. *Science* **2007**, *316*, 582–585. [[CrossRef](#)]
27. Enders, D.; Niemeier, O.; Henseler, A. Organocatalysis by N-heterocyclic carbenes. *Chem. Rev.* **2007**, *107*, 5606–5655. [[CrossRef](#)] [[PubMed](#)]
28. Gaunt, M.J.; Johansson, C.C.; McNally, A.; Vo, N.T. Enantioselective organocatalysis. *Drug Discov. Today* **2007**, *12*, 8–27. [[CrossRef](#)] [[PubMed](#)]
29. MacMillan, D.W. The advent and development of organocatalysis. *Nature* **2008**, *455*, 304–308. [[CrossRef](#)] [[PubMed](#)]
30. Bertelsen, S.; Jorgensen, K.A. Organocatalysis-after the gold rush. *Chem. Soc. Rev.* **2009**, *38*, 2178–2189. [[CrossRef](#)] [[PubMed](#)]
31. Briere, J.F.; Oudeyer, S.; Dalla, V.; Levacher, V. Recent advances in cooperative ion pairing in asymmetric organocatalysis. *Chem. Soc. Rev.* **2012**, *41*, 1696–1707. [[CrossRef](#)]
32. Dalko, P.I. *Comprehensive Enantioselective Organocatalysis*; Wiley-VCH Verlag GbmH & Co. KGaA: Weinheim, Germany, 2013.
33. Serdyuk, O.V.; Heckel, C.M.; Tsogoeva, S.B. Bifunctional primary amine-thioureas in asymmetric organocatalysis. *Org. Biomol. Chem.* **2013**, *11*, 7051–7071. [[CrossRef](#)] [[PubMed](#)]
34. Legros, F.; Oudeyer, S.; Levacher, V. New Developments in Chiral Cooperative Ion Pairing Organocatalysis by Means of Ammonium Oxyanions and Fluorides: From Protonation to Deprotonation Reactions. *Chem. Rec.* **2017**, *17*, 429–440. [[CrossRef](#)]
35. Oudeyer, S.; Levacher, V.; Brière, J.-F. Chiral Quaternary Ammonium Salts in Organocatalysis. In *Quaternary Ammonium Salts in Organocatalysis*; Elsevier: Amsterdam, The Netherlands, 2017; pp. 87–173.
36. Guo, H.; Fan, Y.C.; Sun, Z.; Wu, Y.; Kwon, O. Phosphine Organocatalysis. *Chem. Rev.* **2018**, *118*, 10049–10293. [[CrossRef](#)] [[PubMed](#)]
37. Lopez, S.S.; Nimmagadda, S.K.; Antilla, J.C. Organocatalytic Asymmetric Dearomatization Reactions. In *Asymmetric Dearomatization Reactions*; Wiley-VCH Verlag GmbH: Weinheim, Germany, 2016; pp. 175–206.

38. Schifferer, L.; Stinglhamer, M.; Kaur, K.; Macheño, O.G. Halides as versatile anions in asymmetric anion-binding organocatalysis. *Beilstein J. Org. Chem.* **2021**, *17*, 2270–2286. [\[CrossRef\]](#) [\[PubMed\]](#)
39. Gandhi, S.; Sivasdas, V.; Baire, B. Thiourea–Tertiary Amine Promoted Cascade Catalysis: A Tool for Complexity Generation. *Eur. J. Org. Chem.* **2020**, *2021*, 220–234. [\[CrossRef\]](#)
40. Doyle, A.G.; Jacobsen, E.N. Small-molecule H-bond donors in asymmetric catalysis. *Chem. Rev.* **2007**, *107*, 5713–5743. [\[CrossRef\]](#)
41. Taylor, M.S.; Tokunaga, N.; Jacobsen, E.N. Enantioselective thiourea-catalyzed acyl-mannich reactions of isoquinolines. *Angew. Chem. Int. Ed.* **2005**, *44*, 6700–6704. [\[CrossRef\]](#)
42. Schafer, A.G.; Wieting, J.M.; Fisher, T.J.; Mattson, A.E. Chiral silanediols in anion-binding catalysis. *Angew. Chem. Int. Ed.* **2013**, *52*, 11321–11324. [\[CrossRef\]](#)
43. Chandrasekhar, V.; Boomishankar, R.; Nagendran, S. Recent developments in the synthesis and structure of organosilanols. *Chem. Rev.* **2004**, *104*, 5847–5910. [\[CrossRef\]](#)
44. Zurro, M.; Asmus, S.; Bamberger, J.; Beckendorf, S.; Garcia Mancheno, O. Chiral Triazoles in Anion-Binding Catalysis: New Entry to Enantioselective Reissert-Type Reactions. *Chemistry* **2016**, *22*, 3785–3793. [\[CrossRef\]](#)
45. Ray Choudhury, A.; Mukherjee, S. Enantioselective dearomatization of isoquinolines by anion-binding catalysis en route to cyclic alpha-aminophosphonates. *Chem. Sci.* **2016**, *7*, 6940–6945. [\[CrossRef\]](#) [\[PubMed\]](#)
46. Matador, E.; Iglesias-Sigüenza, J.; Monge, D.; Merino, P.; Fernandez, R.; Lassaletta, J.M. Enantio- and Diastereoselective Nucleophilic Addition of N-tert-Butylhydrazones to Isoquinolinium Ions through Anion-Binding Catalysis. *Angew. Chem. Int. Ed.* **2021**, *60*, 5096–5101. [\[CrossRef\]](#) [\[PubMed\]](#)
47. De, C.K.; Mittal, N.; Seidel, D. A dual-catalysis approach to the asymmetric Steglich rearrangement and catalytic enantioselective addition of O-acylated azlactones to isoquinolines. *J. Am. Chem. Soc.* **2011**, *133*, 16802–16805. [\[CrossRef\]](#) [\[PubMed\]](#)
48. Zurro, M.; Asmus, S.; Beckendorf, S.; Muck-Lichtenfeld, C.; Mancheno, O.G. Chiral helical oligotriazoles: New class of anion-binding catalysts for the asymmetric dearomatization of electron-deficient N-heteroarenes. *J. Am. Chem. Soc.* **2014**, *136*, 13999–14002. [\[CrossRef\]](#)
49. Fischer, T.; Duong, Q.N.; Garcia Mancheno, O. Triazole-Based Anion-Binding Catalysis for the Enantioselective Dearomatization of N-Heteroarenes with Phosphorus Nucleophiles. *Chemistry* **2017**, *23*, 5983–5987. [\[CrossRef\]](#)
50. Duong, Q.-N.; Schifferer, L.; García Mancheno, O. Nucleophile Screening in Anion-Binding Reissert-Type Reactions of Quinolines with Chiral Tetrakis(triazole) Catalysts. *Eur. J. Org. Chem.* **2019**, *2019*, 5452–5461. [\[CrossRef\]](#)
51. Gomez-Martinez, M.; Del Carmen Perez-Aguilar, M.; Piekarski, D.G.; Daniliuc, C.G.; Garcia Mancheno, O. N,N-Dialkylhydrazones as Versatile Umpolung Reagents in Enantioselective Anion-Binding Catalysis. *Angew. Chem. Int. Ed.* **2021**, *60*, 5102–5107. [\[CrossRef\]](#)
52. Yamaoka, Y.; Miyabe, H.; Takemoto, Y. Catalytic enantioselective petasis-type reaction of quinolines catalyzed by a newly designed thiourea catalyst. *J. Am. Chem. Soc.* **2007**, *129*, 6686–6687. [\[CrossRef\]](#)
53. Garcia Mancheno, O.; Asmus, S.; Zurro, M.; Fischer, T. Highly Enantioselective Nucleophilic Dearomatization of Pyridines by Anion-Binding Catalysis. *Angew. Chem. Int. Ed.* **2015**, *54*, 8823–8827. [\[CrossRef\]](#)
54. Bertuzzi, G.; Sinisi, A.; Caruana, L.; Mazzanti, A.; Fochi, M.; Bernardi, L. Catalytic Enantioselective Addition of Indoles to Activated N-Benzylpyridinium Salts: Nucleophilic Dearomatization of Pyridines with Unusual C-4 Regioselectivity. *ACS Catal.* **2016**, *6*, 6473–6477. [\[CrossRef\]](#)
55. Fischer, T.; Bamberger, J.; Mancheno, O.G. Asymmetric nucleophilic dearomatization of diazaarenes by anion-binding catalysis. *Org. Biomol. Chem.* **2016**, *14*, 5794–5802. [\[CrossRef\]](#)
56. Kaur, K.; Humbrias-Martin, J.; Hoppmann, L.; Fernandez-Salas, J.A.; Daniliuc, C.G.; Aleman, J.; Mancheno, O.G. Enantioselective vinylogous-Mukaiyama-type dearomatization by anion-binding catalysis. *Chem. Commun.* **2021**, *57*, 9244–9247. [\[CrossRef\]](#)
57. Melchiorre, P.; Marigo, M.; Carlone, A.; Bartoli, G. Asymmetric aminocatalysis—gold rush in organic chemistry. *Angew. Chem. Int. Ed.* **2008**, *47*, 6138–6171. [\[CrossRef\]](#)
58. Frisch, K.; Landa, A.; Saaby, S.; Jorgensen, K.A. Organocatalytic diastereo- and enantioselective annulation reactions—construction of optically active 1,2-dihydroisoquinoline and 1,2-dihydrophthalazine derivatives. *Angew. Chem. Int. Ed.* **2005**, *44*, 6058–6063. [\[CrossRef\]](#) [\[PubMed\]](#)
59. Mengozzi, L.; Gualandi, A.; Cozzi, P.G. A highly enantioselective acyl-Mannich reaction of isoquinolines with aldehydes promoted by proline derivatives: An approach to 13-alkyl-tetrahydroprotoberberine alkaloids. *Chem. Sci.* **2014**, *5*, 3915–3921. [\[CrossRef\]](#)
60. Berti, F.; Malossi, F.; Marchetti, F.; Pineschi, M. A highly enantioselective Mannich reaction of aldehydes with cyclic N-acyliminium ions by synergistic catalysis. *Chem. Commun.* **2015**, *51*, 13694–13697. [\[CrossRef\]](#) [\[PubMed\]](#)
61. Sun, S.; Mao, Y.; Lou, H.; Liu, L. Copper(II)/amine synergistically catalyzed enantioselective alkylation of cyclic N-acyl hemiaminals with aldehydes. *Chem. Commun.* **2015**, *51*, 10691–10694. [\[CrossRef\]](#) [\[PubMed\]](#)
62. Volla, C.M.; Fava, E.; Atodiresei, I.; Rueping, M. Dual metal and Lewis base catalysis approach for asymmetric synthesis of dihydroquinolines and the alpha-arylation of aldehydes via N-acyliminium ions. *Chem. Commun.* **2015**, *51*, 15788–15791. [\[CrossRef\]](#)
63. Mengozzi, L.; Gualandi, A.; Cozzi, P.G. Organocatalytic Stereoselective Addition of Aldehydes to Acylquinolinium Ions. *Eur. J. Org. Chem.* **2016**, *2016*, 3200–3207. [\[CrossRef\]](#)

64. Song, X.; Yan, R.J.; Du, W.; Chen, Y.C. Asymmetric Dearomative Cascade Multiple Functionalizations of Activated N-Alkylpyridinium and N-Alkylquinolinium Salts. *Org. Lett.* **2020**, *22*, 7617–7621. [\[CrossRef\]](#)
65. Bertuzzi, G.; Sinisi, A.; Pecorari, D.; Caruana, L.; Mazzanti, A.; Bernardi, L.; Fochi, M. Nucleophilic Dearomatization of Pyridines under Enamine Catalysis: Regio-, Diastereo-, and Enantioselective Addition of Aldehydes to Activated N-Alkylpyridinium Salts. *Org. Lett.* **2017**, *19*, 834–837. [\[CrossRef\]](#)
66. Yan, R.J.; Xiao, B.X.; Ouyang, Q.; Liang, H.P.; Du, W.; Chen, Y.C. Asymmetric Dearomative Formal [4 + 2] Cycloadditions of N,4-Dialkylpyridinium Salts and Enones To Construct Azaspiro[5.5]undecane Frameworks. *Org. Lett.* **2018**, *20*, 8000–8003. [\[CrossRef\]](#)
67. Benfatti, F.; Benedetto, E.; Cozzi, P.G. Organocatalytic stereoselective alpha-alkylation of aldehydes with stable carbocations. *Chem. Asian J.* **2010**, *5*, 2047–2052. [\[CrossRef\]](#)
68. Liang, T.; Xiao, J.; Xiong, Z.; Li, X. Organocatalytic asymmetric 1,4-addition of aldehydes to acridiniums catalyzed by a diarylprolinol silyl ether. *J. Org. Chem.* **2012**, *77*, 3583–3588. [\[CrossRef\]](#)
69. Zhang, B.; Xiang, S.K.; Zhang, L.H.; Cui, Y.; Jiao, N. Organocatalytic asymmetric intermolecular dehydrogenative alpha-alkylation of aldehydes using molecular oxygen as oxidant. *Org. Lett.* **2011**, *13*, 5212–5215. [\[CrossRef\]](#)
70. Guo, C.; Fleige, M.; Janssen-Muller, D.; Daniliuc, C.G.; Glorius, F. Switchable selectivity in an NHC-catalysed dearomatizing annulation reaction. *Nat. Chem.* **2015**, *7*, 842–847. [\[CrossRef\]](#)
71. Wang, Y.; Qu, L.B.; Wei, D. Prediction on the Origin of Selectivities in Base-controlled Switchable NHC-catalyzed Transformations. *Chem. Asian J.* **2019**, *14*, 293–300. [\[CrossRef\]](#) [\[PubMed\]](#)
72. Zhang, P.; Zhou, Y.; Han, X.; Xu, J.; Liu, H. N-Heterocyclic Carbene Catalyzed Enantioselective [3 + 2] Dearomatizing Annulation of Saturated Carboxylic Esters with N-Iminoisoquinolinium Ylides. *J. Org. Chem.* **2018**, *83*, 3879–3888. [\[CrossRef\]](#)
73. Xu, J.H.; Zheng, S.C.; Zhang, J.W.; Liu, X.Y.; Tan, B. Construction of Tropane Derivatives by the Organocatalytic Asymmetric Dearomatization of Isoquinolines. *Angew. Chem. Int. Ed.* **2016**, *55*, 11834–11839. [\[CrossRef\]](#) [\[PubMed\]](#)
74. Wang, Y.; Wu, Q.-Y.; Lai, T.-H.; Zheng, K.-J.; Qu, L.-B.; Wei, D. Prediction on the origin of selectivities of NHC-catalyzed asymmetric dearomatization (CADA) reactions. *Catal. Sci. Technol.* **2019**, *9*, 465–476. [\[CrossRef\]](#)
75. Flanagan, D.M.; Rovis, T. Enantioselective N-heterocyclic carbene-catalyzed nucleophilic dearomatization of alkyl pyridiniums. *Chem. Sci.* **2017**, *8*, 6566–6569. [\[CrossRef\]](#) [\[PubMed\]](#)
76. Wang, Y.; Qu, L.B.; Lan, Y.; Wei, D. Origin of Regio- and Stereoselectivity in the NHC-catalyzed Reaction of Alkyl Pyridinium with Aliphatic Enal. *ChemCatChem* **2019**, *12*, 1068–1074. [\[CrossRef\]](#)
77. Di Carmine, G.; Ragno, D.; Bortolini, O.; Giovannini, P.P.; Mazzanti, A.; Massi, A.; Fogagnolo, M. Enantioselective Dearomatization of Alkylpyridiniums by N-Heterocyclic Carbene-Catalyzed Nucleophilic Acylation. *J. Org. Chem.* **2018**, *83*, 2050–2057. [\[CrossRef\]](#)
78. McLaughlin, C.; Bitai, J.; Barber, L.J.; Slawin, A.M.; Smith, A.D. Catalytic enantioselective synthesis of 1,4-dihydropyridines via the addition of C(1)-ammonium enolates to pyridinium salts. *Chem. Sci.* **2021**, *12*, 12001–12011. [\[CrossRef\]](#)
79. Yuan, C.; Zhou, L.; Xia, M.; Sun, Z.; Wang, D.; Guo, H. Phosphine-Catalyzed Enantioselective [4 + 3] Annulation of Allenolates with C,N-Cyclic Azomethine Imines: Synthesis of Quinazoline-Based Tricyclic Heterocycles. *Org. Lett.* **2016**, *18*, 5644–5647. [\[CrossRef\]](#) [\[PubMed\]](#)
80. Chen, D.; Xu, G.; Zhou, Q.; Chung, L.W.; Tang, W. Practical and Asymmetric Reductive Coupling of Isoquinolines Templated by Chiral Diborons. *J. Am. Chem. Soc.* **2017**, *139*, 9767–9770. [\[CrossRef\]](#)